RESEARCH ARTICLE

Molecular Changes in Normal Appearing White Matter in Multiple Sclerosis are Characteristic of Neuroprotective Mechanisms Against Hypoxic Insult

Ursula Graumann[1]; Richard Reynolds[2]; Andreas J. Steck[1]; Nicole Schaeren-Wiemers[1]

[1] Neurobiology, Department of Research and Neurology, University Hospital Basel, Switzerland.
[2] Department of Neuroinflammation, Division of Neuroscience, Imperial College London, Charing Cross Campus, United Kingdom.

Multiple sclerosis is a chronic inflammatory disease of the CNS leading to focal destruction of myelin, still the earliest changes that lead to lesion formation are not known. We have studied the gene-expression pattern of 12 samples of normal appearing white matter from 10 post-mortem MS brains. Microarray analysis revealed upregulation of genes involved in maintenance of cellular homeostasis, and in neural protective mechanisms known to be induced upon ischemic preconditioning. This is best illustrated by the upregulation of the transcription factors such as HIF-1α and associated PI3K/Akt signalling pathways, as well as the upregulation of their target genes such as VEGF receptor 1. In addition, a general neuroprotective reaction against oxidative stress is suggested. These molecular changes might reflect an adaptation of cells to the chronic progressive pathophysiology of MS. Alternatively, they might also indicate the activation of neural protective mechanisms allowing preservation of cellular and functional properties of the CNS. Our data introduce novel concepts of the molecular pathogenesis of MS with ischemic preconditioning as a major mechanism for neuroprotection. An increased understanding of the underlying mechanisms may lead to the development of new more specific treatment to protect resident cells and thus minimize progressive oligondendrocyte and axonal loss.

Brain Pathol 2003;13:554-573.

Introduction

The study of the pathogenetic mechanisms involved in lesion formation in multiple sclerosis (MS) is complicated by the multifactorial nature of disease susceptibility. Heterogeneity of clinical disease course and the variety of the cellular pathology seen at post-mortem further complicate the picture. To date most of the studies designed to elucidate molecular mechanisms of lesion formation have focused on changes occurring in chronic demyelinated lesions (24, 25). In contrast, very little is known concerning the molecular changes taking place in the normal appearing white matter (NAWM) in MS, where one might expect to see the earliest changes relating to new lesion formation.

Magnetic resonance imaging studies (MRI) have demonstrated that there are abnormalities in the NAWM in a majority of MS cases (13). Axonal injury, blood brain barrier changes and reactive astro- and micro-gliosis have been reported (2, 14, 41). At the molecular level, however, little is known about the mechanisms leading to lesion formation and whether protective mechanisms involved in maintaining brain homeostasis could be exploited to develop new treatments.

Here, we have examined the molecular alterations that occur in NAWM of post-mortem tissues from MS patients in order to identify adaptive molecular changes. Thorough neuropathological and clinical examination of each MS and control case, and histological characterization of each analyzed brain tissue sample were used for validation and interpretation of the microarray analysis.

Material and Methods

Tissue collection and characterization. MS and control tissue samples were obtained from the UK MS Tissue Bank at Imperial College (UK Multicentre Research Ethics Committee, MREC/02/2/39). Tissue blocks (2 cm $\times$ 2 cm $\times$ 1 cm, Figure 1D) representing normal (non-neurological) control white matter and normal appearing MS white matter (NAWM) were analyzed to exclude additional pathological alterations. Control tissue blocks were taken from corresponding brain areas (Table 1). Tissue blocks were snap frozen and

Corresponding author:
Nicole Schaeren-Wiemers, Neurobiology, Department of Research, Pharmacenter, Klingelbergstrasse 50, CH-4056 Basel, Switzerland (Email: Nicole.Schaeren-Wiemers@unibas.ch)

MS	Brain Area	PMD	Age	Sex	Array/LC	Cause of death	General cortical pathology	MS	DD
MS1[1]	A3B2 Fcx NAWM	8h	56	f	I, III	Bilateral basal pneumonia	Demyelinated lesions in subcortical wm and gm, little m/m activation.	SP	31y
MS1[2]	A3D1 Fcx NAWM				I, II, III, LC				
MS2	P5C4 Ocx NAWM	16h	58	f	I, LC	Peritonitis	Multiple lesions in subcortical WM, some shadow plaques.	PP	22y
MS3[1]	A4B4 Fcx NAWM	18h	76y	f	I, II, III, LC	Myocardial infarction	Demyelinated lesions in subcortical wm and shadow plaques.	SP	>14y
MS3[2]	A4C4 Ccx NAWM				I				
MS5[1]	A3C2 Fcx NAWM	6h	58y	f	I, II, III, LC	Broncho-pneumonia	Numerous subcortical lesions from mm to cm size throughout hemispheres.	PP	21y
MS5[2]	A3C7 Fcx NAWM				I, II, III, LC				
MS10	A4D3 Fcx NAWM	11h	69y	f	I, II, LC	Acute pyelonephritis	Number of subcortical wm and gm lesions, cm size, some remyelination.	PP	31y
MS12	P1A4 Fcx NAWM	9h	78y	f	I, LC	Lung infection	Small and large demyelinated lesions, some remyelination in all cortical lobes, some inflammation.	PP	31y
MS18	P3B3 Ocx NAWM	5h	78y	f	I, LC	Broncho-carcinoma	No lesions in cerebral cortex, lesions only in medulla, brainstem and spinal cord.	RR SP	42y
MS20	P3B3 Ocx NAWM	13h	66y	f	I, LC	Aspiration pneumonia	Demyelinated lesions with evidence of remyelination in frontal cx, few hypoxic neurons.	SP	30y
MS25	A3B2 Fcx NAWM	22h	54y	f	LC	Broncho-pneumonia	Many demyelinated lesions throughout hemispheres, no inflammation	SP	20y
MS26	Tcx NAWM	6h	83y	f	I, II, III	Myocardial infarction	Multiple, small (4-5mm) chronic demyelinated lesions in GM and WM throughout hemispheres, no inflammation.	Silent MS	-
Controls									
CLo6[1]	P3D3Ocx WM	21h	73y	m	I, II, III, LC	Heart attack	Occasional fresh hypoxic nerve cell changes in some cortical areas.		
CLo6[2]	A2C3 Fcx WM				I				
CLo7	A3C5 Fcx WM	26h	77y	m	2xI, LC	Lung cancer	Gliosis in some wm areas.		
CLo8	P1B4 Pcx WM	18h	64y	f	I, II, LC	Cardiac failure	Occasional presence of hypoxic neurons and perineuronal oedema.		
CBS1	Pcx WM	15h	70y	m	I, II, III, LC	Myocardial infarct	Few acute hypoxic neurons in neocortex.		
CBS2	Fcx WM	16h	66y	m	I, II, III, LC	Broncho-carcinoma	No metastases in brain.		
CBS4	Ccx WM	10h	69y	m	3x I, LC	Myocardial infarct	No pathological alterations.		
CBS5	Tcx WM	22h	59y	f	I, II, III, LC	Acute pancreatitis	Minor neurodegenerative changes in the entorhinal cortex.		

Table 1. *Summary of clinical data.* Clinical and pathological information concerning the 10 MS and 7 control subjects studied are shown. 2 separate samples of brain tissues were analyzed from MS1, MS3, MS5 and CLo6. All brain tissues were rapidly frozen after retrieval and their RNA integrity verified. Full CNS pathological characterization was performed on all cases. All NAWM and control white matter samples were derived from sub-cortical white matter. Hybridization analysis was performed on the Atlas Human 1.2 Arrays I, II or III and by quantitative RT-PCR (LightCycler) as indicated. Abbreviations: NAWM, normal appearing white matter; wm, white matter; Fcx, frontal cortex; Ocx, occipital cortex; Ccx, cingulated cortex; Tcx, temporal cortex; Pcx, pariental cortex; f, female; m, male; LC, LightCycler; SP, secondary progressive; PP, primary progressive.

stored at -80°C. Additional tissue samples were collected at the Department of Pathology, University Hospital Basel (Ethics Committee of the University Hospital Basel). All brains were routinely screened by a neuropathologist to confirm diagnosis of MS and to exclude confounding pathologies. This information, together with a clinical summary of disease course and patient specific data are summarized in Table 1. Before extraction of RNA, immunohistochemical analysis for PLP (kindly provided by K.-A. Nave, Göttingen),

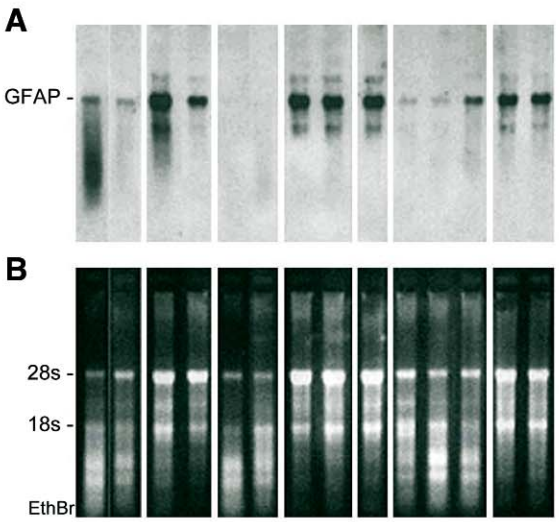

C

Lane	Patient	Tissue	p.m.	Age	RNA
1	MS4	P5C6 P2C2	19h	74ys	Deg
2	MS3	A4D6 A4B4	18h	78ys	Intact
3	MS6	P6D3 P6D5	17h	45ys	Deg
4	MS1	P4C2 A3B2	8h	56ys	Intact
5	MS5	A3B6	6h	58ys	Intact
6+7	CLo2	A1B3 A3B2	10h	95ys	Deg
8	CLo3	A2B3	9h	85ys	Deg
9+10	CBS	wm Cer	4h	44ys	Intact

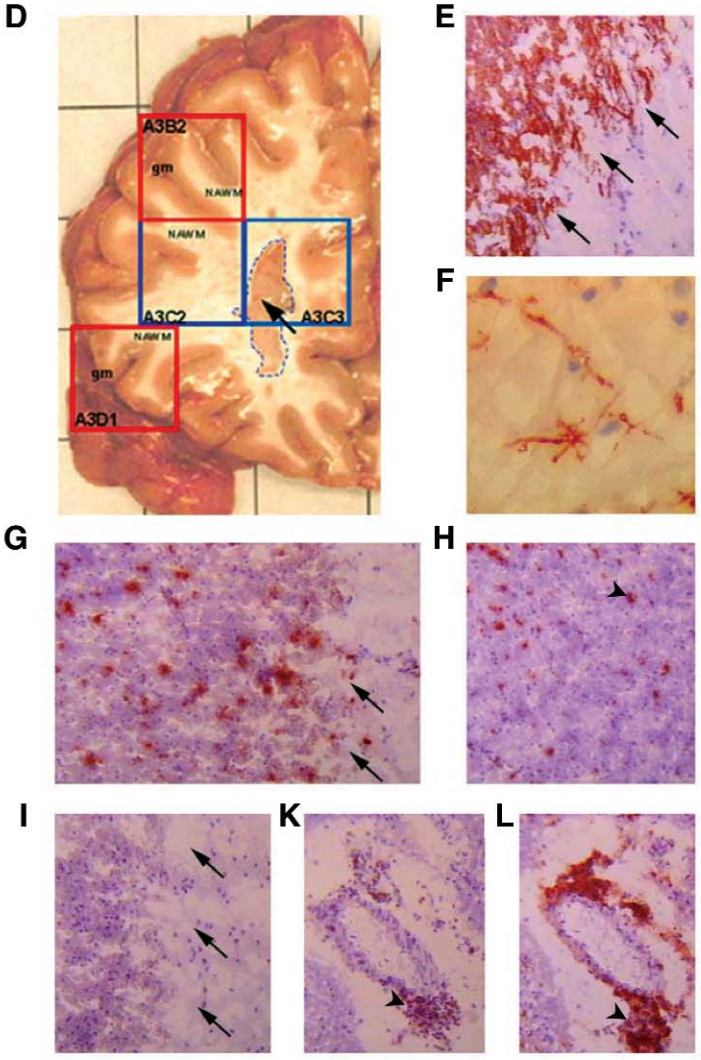

MOG, GFAP (Dako), CD68 and CD3 (Dako) expression was performed on cryostat sections (10 μm) from each tissue block.

Total RNA preparation and Northern blot analysis. Total RNA isolation was performed by homogenization in guanidinium thiocyanate followed by a CsCl ultracentrifugation (5). This protocol provides the highest purity and quantity of total RNA from human brain tissues. Freshly isolated RNA was checked for integrity and for several representative transcripts by Northern blot analysis using DIG-labeled cRNA probes as described previously (36).

Atlas™ cDNA Expression Array hybridization. The Clontech Atlas™ cDNA Expression Array 1.2 (I-III) contains 3528 selected cDNA sequences arrayed on 3 different nylon membranes (1176 per array). Radiolabeled single stranded cDNAs were generated by reverse transcription of 4 μg total RNA with the gene-specific primer sets for each gene represented on the array and hybridization was performed following the manufacture's protocol (Clontech). Hybridization signals were detected and visualized with the phosphoimaging system (Molecular Dynamics). Array I was hybridized with 11 MS and 8 control samples, Array II with 7 MS and 5 control samples and Array III with 6 MS and 4 control samples (Table 1).

Data analysis and interpretation. Quantification of differential hybridization signal intensities was achieved with the AtlasImage™ 2.0 software program. For comparing the differential expression pattern between different experiments, we used the gene for the 60S ribosomal protein L13A (accession number X56932) for normalization of Array I and III and for the RNA binding protein fus (accession number X71428) for Array II. Hybridization signal intensities, which were in 75% of the cases below 4000 pixels were excluded from our analysis. This was the case for 595 cDNA sequences on array I. Normalized hybridization intensities from each MS sample were compared with the corresponding one from each control to provide fold-changes (ratio). Boxplot analysis of fold changes (ratios) were used to examine their distribution in one variable case, either MS versus all controls or one control case versus all MS. The median value of fold changes for each MS was evaluated against all controls. Three hundred thirty-four genes had median values of fold changes either below 0.7 (down-regulated in MS) or higher than 1.5 in more than half of the MS samples (Table 2), and these genes were used for further statistical analysis.

Quantitative RT-PCR. Real-time RT-PCR was performed using the LightCycler system (Roche). Primer sequences were either provided by Clontech or designed from unique site over exon-intron junctions to prevent amplification of genomic DNA. Real-time RT-PCR was performed according manufacturer's protocol (Roche). RNA amounts were calculated with relative standard curves for all mRNAs of interest and 60S ribosomal protein LA13 for normalization.

In situ hybridization. Generation of digoxigenin-labelled cRNA probes and in situ hybridization on cryosections of freshly frozen tissue were performed as previously described (36).

Statistics. Hierarchical cluster analysis was performed with the program "Cluster" and "TreeView" from Michael Eisen (11). To assess sample clusters the median values for each MS were imported into "Cluster" and converted into $\log_2$ values (Figure 2A). According to the cluster analysis from the MS tissues all fold changes of MS versus every control (ratios) were sorted into the data sheet and hierarchical gene cluster analysis was performed (Figure 2B). Individual fold changes (ratios) of each MS sample are shown as medians (Table 2). Statistical significance is expressed by *p*-values generated by the non-parametric Mann-Whitney U-Test. For this, the hybridization signal intensities were normalized to one of the control samples.

Figure 1. (Opposing page) *Molecular and histopathological characterization of brain tissues.* Northern blot analysis for GFAP mRNA expression was performed with digoxigenin-labelled cRNA probes (**A**) for each tissue block for verification of the RNA integrity. 2mg totRNA was loaded per lane and stained with ethidium bromide (**B**). For illustration, tot RNA from some tissue blocks are shown (**C** for details). Control RNA was loaded from white matter (corpus callosum) and from cerebellum. Neuropathological characterization of the different cases revealed that most of the detected lesions were inactive chronic demyelinated lesions (**D**). In some lesions MOG positive oligodendrocytes were also observed (**F**). Immunohistochemistry of each tissue block (**D**) was performed to distinguish blocks with NAWM (red) from ones with lesions (blue) and to identify grey matter regions. Analysis of one tissue block is shown for PLP (E), CD68 (**G, H, L**) and CD3 (**I, K**). Arrows (in **E, G, I**) point to the lesion border (**D**). For the microarray analysis NAWM from tissue blocks without lesions (**D**, red) were dissected, excluding areas of grey matter. Control tissues were analyzed in comparable manner.

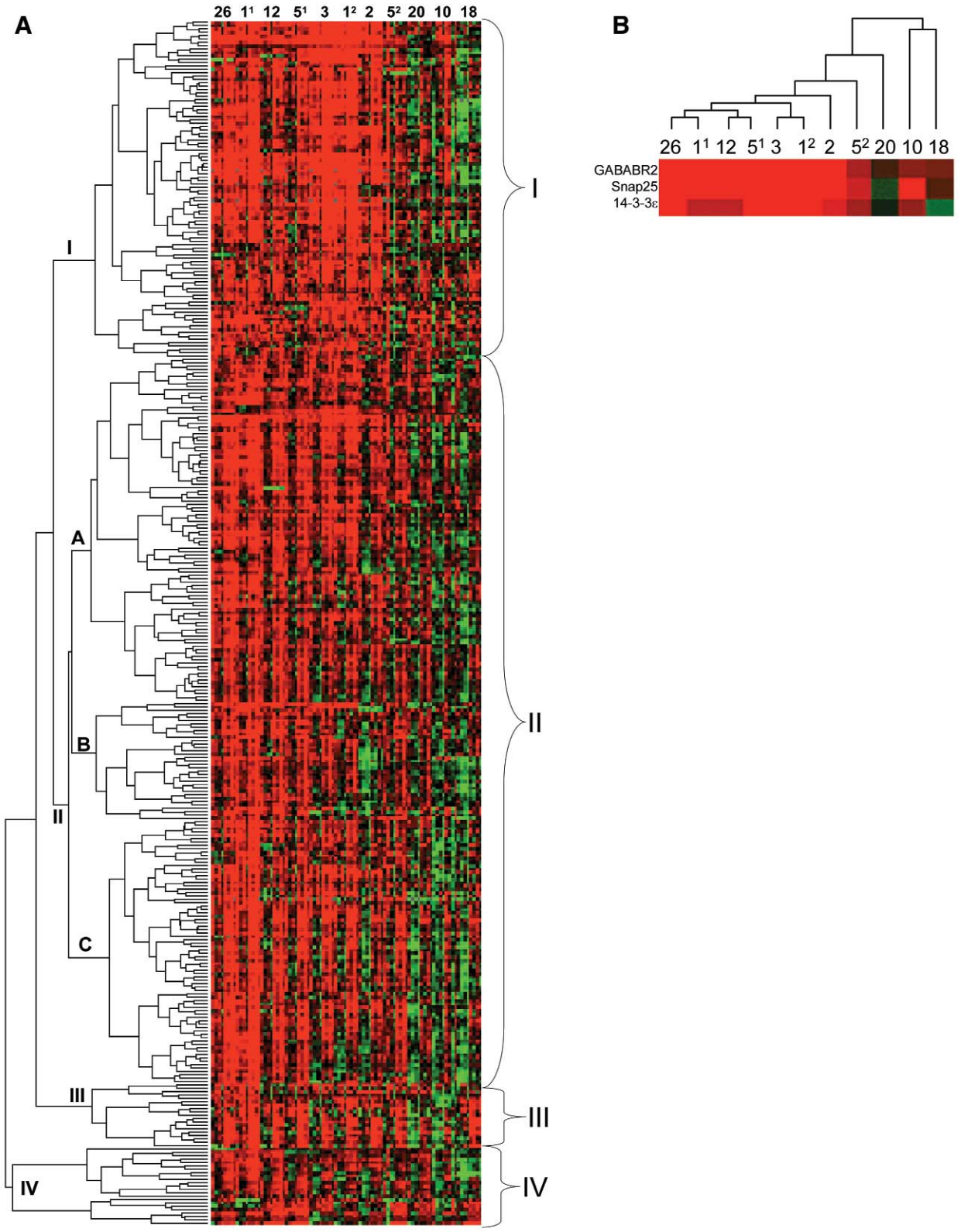
A
26 1¹ 12 5¹ 3 1² 2 5² 20 10 18
I
II
III
IV
A
B
C
B
26 1¹ 12 5¹ 3 1² 2 5² 20 10 18
GABABR2
Snap25
14-3-3ε

Results

Molecular and histopathological characterization of tissues obtained from post mortem MS and control cerebral cortex. Isolation and characterization of 52 tissue blocks from the cerebral cortex (37 MS and 15 controls) from 38 different patients (26 MS and 12 controls), with a post-mortem delay (PMD) of less than 26 hours, showed that in 24 out of 38 cases RNA was preserved (Figure 1A, B show a selection of representative cases). Although, there was a large variation in PMD time (Table 1), we did not identify a correlation between PMD and degree of RNA degradation (Figure 1C).

Data obtained from the analysis of gene array hybridizations are best interpreted together with a detailed knowledge of the cellular composition and pathological changes in the particular tissue sample being studied. Considerable variations occur from region to region depending on whether a demyelinated lesion is close to or distant from the NAWM block. Therefore, we performed an immunohistochemical analysis of each tissue block in order to identify white and grey matter regions and to exclude demyelinating lesions (Figure 1D). We used antibodies against proteolipid protein (PLP, Figure 1E) and myelin-oligodendrocyte glycoprotein (MOG, Figure 1F) for myelinated fibers, glial fibrillary acidic protein (GFAP, not shown) for reactive astrocytes, CD68 for activated macrophages and microglia (Figure 1G, H, L) and CD3 for the identification of infiltrating T-lymphocytes (Figure 1I, K). From this analysis we chose only NAWM tissue from tissue blocks without any histological evidence of demyelinating lesions or inflammatory activity. In subcortical NAWM tissues, only few CD3 positive lymphocytes were observed within blood vessels (Figure 1K, arrowhead) and very seldom within the white or grey matter (Figure 1I). In most of the NAWM tissues we detected a considerable number of reactive CD68 positive cells throughout the tissues (Figure 1H, arrowhead), occasionally accumulated around blood vessels (Figure 1L, arrowhead).

Microarray analysis of differentially expressed genes in NAWM of MS tissues. We performed differential screening with 11 total RNA samples from subcortical NAWM of 9 different MS cases and 8 total RNA samples from subcortical white matter of 7 control cases (Table 1). Hierarchical cluster analysis with the programs "Cluster" and "TreeView" (11) was used for identifying groups of genes with a common expression pattern within the MS samples (Figure 2A). This revealed 4 major gene clusters representing analogous differential expression patterns in NAWM tissues. Genes identified to be differentially expressed in MS NAWM are listed according to their gene cluster (Table 2). The median of fold changes for each gene for each MS sample is given and similarities as well as differences illustrated. We also used hierarchical cluster analysis to group experimental samples on the basis of similarities in their expression pattern: this revealed one major group within the MS cases (Figure 2B). The cluster analysis illustrates a molecular portrait of both similarities and differences in expression patterns among the MS cases. For example, the expression pattern profile of MS18 represented a control profile rather than a MS (Table 2). This is in line with the neuropathological observation that MS18 had no cortical lesions (Table 1). From the cases MS1 and MS5 we have used two NAWM tissue blocks from different brain regions. In both cases comparable results were obtained. In the case of MS1 both tissue samples showed strong overlapping differential expression patterns (Table 2, MS1 A3B2 and MS1 A3D1), whereas in the case of MS5 differential expression of tissue block A3C7 was more modest than of that of A4B4. Overall, the cluster analysis did not show a difference between primary and secondary progressive MS.

Quantitative RT-PCR analysis. In order to verify the array data we performed quantitative RT-PCR on several selected genes (Figure 3A). This analysis is in excellent agreement with the corresponding array results, using Snap25 (synaptosomal associated protein 25), MAL (myelin and lymphocyte protein), MOG and MAG (myelin associated glycoprotein) as examples (Figure

Figure 2. (Opposing page) *Hierarchical cluster.* Cluster analysis was performed to sort genes by similarities in their expression pattern within MS samples compared to each control, which revealed 4 clusters (A). For each gene 88 comparisons (11 MS versus 8 controls) are depicted in color-coded squares representing each fold ratio. Comparisons to each control were arranged in the following order: CBS1, 2, 4, 5, CLo6[1], 6[2], 7, 8 from left to right. This pattern shows the heterogeneity between controls. Red shows upregulation, whereas green downregulation. Genes are listed in Table 2 accordingly. Hierarchical cluster analysis to group MS samples (median value versus all controls) on the basis of similarities in their expression pattern is shown in B (GABABR2, Snap25 and 14-3-3 are shown as example). Note, that the differential expression pattern of MS26, 1, 5, 3, 2 are very similar, whereas MS20, 18 and 10 show a distinct pattern.

A

Quantitative RT-PCR analysis

		MS25	MS12	MS5/1	MS5/2	MS3	MS1/2	MS2	MS20	MS10	MS18	*P*-value
Snap25	LC	22.5	10.4	14.0	6.7	66.5	77.0	10.3	1.7	7.8	2.0	0.001
	Array	n.d.	5.5	6.2	2.9	13.3	12.7	6.3	0.9	4.3	1.5	0.002
HSP70.1	LC	1.1	4.1	0.7	0.6	0.6	0.8	6.0	2.2	1.9	13.0	0.329
	Array	n.d.	0.9	0.4	0.4	0.6	0.8	1.6	1.2	0.8	1.7	0.355
MAL	LC	2.4	2.6	2.4	2.9	2.0	2.2	0.7	1.9	1.2	1.7	0.011
	Array	n.d.	1.6	2.0	1.8	1.4	1.7	1.0	1.1	0.7	1.2	0.076
MAG	LC	2.9	3.6	2.8	2.6	1.4	1.7	0.6	1.9	1.6	1.0	0.118
	Array	n.d.	1.4	1.6	1.3	1.2	1.3	0.5	1.2	0.8	0.8	0.539
MOG	LC	1.0	1.6	1.5	1.5	0.7	0.8	0.4	1.1	0.9	1.1	0.626
	Array	n.d.	1.4	1.5	1.3	1.0	1.1	0.7	1.1	0.5	1.0	0.488
MBP	LC	1.3	1.5	0.3	0.5	0.3	0.3	0.5	5.4	2.6	0.8	0.435
MOBP	LC	1.0	2.7	1.2	1.1	0.4	0.5	0.7	2.7	2.2	1.0	0.380
CNP	LC	2.4	3.9	2.0	1.5	1.0	1.3	0.5	2.8	1.5	1.2	0.242
PLP	LC	2.9	2.6	1.9	1.4	0.9	1.3	0.6	1.8	1.4	0.9	0.118
GFAP	LC	2.6	1.4	2.2	1.8	1.3	1.2	1.1	1.0	0.8	1.6	0.143
NSE	LC	11.0	6.7	6.0	3.7	4.1	3.9	2.9	2.2	2.8	2.0	0.001

B

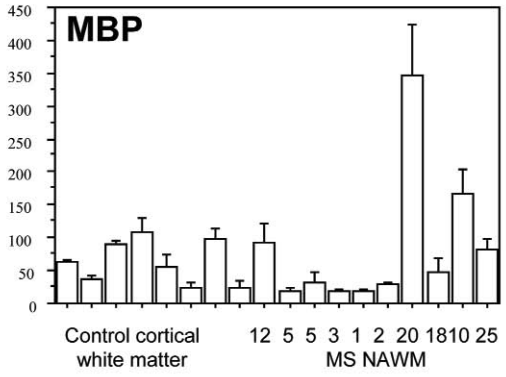

C

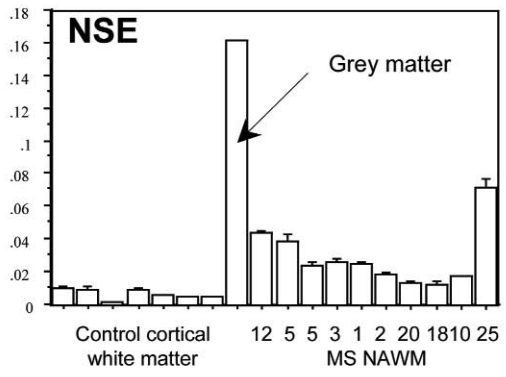

Figure 3. *Quantitative RT-PCR analysis.* Quantitative RT-PCR analysis (**A**) shows the differential gene expression of selected genes: the values represent the medians of all ratios of one MS versus all controls. The result from Real-Time-PCR (LC) and Array 1.2 I are compared for Snap25, HSP70.1, MAL, MAG and MOG. In addition, hybridization signals at saturated levels (MBP, PLP and GFAP) and genes not represented on the Array I (MOBP, CNP and NSE) were analyzed. Red shows upregulation, whereas green down-regulation. Statistical significance is expressed as p-value; values below 0.05 are shown in yellow. The expression intensities measured by LightCycler analysis of MBP (**B**) and NSE (**C**) for each case are shown as example. (LC, lightCycler, n.d., not done).

3A). However, the RT-PCR results revealed a greater fold difference, indicating that differential expression is under- than overestimated from the array analysis. This was especially the case for genes expressed at high levels such as Snap25, Hsp70.1 (heat shock protein 70.1), MBP, PLP and GFAP, due to the saturation limit of the hybridization signal. In addition, we analyzed the expression level of two additional oligodendrocyte specific genes, MOBP (myelin/oligodendrocyte-specific protein) and CNP (2′,3′-cyclic nucleotide 3′-phosphodiesterase), which were not present on array I (Figure 3A). In view of the fact that many of the upregulated genes are thought to be predominantly expressed in neurons, we analyzed the expression level of the neuronal house keeping gene neuron specific enolase (NSE), which turned out to be upregulated in all MS cases (Figure 3A, C).

Differential expression of genes in NAWM. A number of genes were clearly upregulated in MS NAWM in the majority of the cases. These changes represent alterations in intracellular "housekeeping" metabolism as well as in receptor mediated signalling pathways and transcriptional regulation. The cellular specificity for many of the identified genes is not known, and we have to assume that some genes are expressed in several cell types. For this reason, we first analyzed the data with respect to cell type and then used hierarchical cluster analysis for identifying groups of genes with a common expression pattern (Figure 2A; Table 2). It should be noted that downregulation of genes has been observed but only in single cases (Table 2; Figures 2, 3).

One point of interest was the expression pattern of oligodendrocyte specific genes. Although from a morphological point of view myelin appeared normal, myelin maintenance was altered at the transcriptional level. A striking feature was the downregulation of MBP in many cases (Figure 3A, B). However, in 2 cases (MS 20 and 10), strong upregulation was detected, a feature consistent with remyelinating activity. Remyelinated areas (eg, shadow plaques) were observed in both of these cases (Table 1). MOBP showed a comparable expression pattern to MBP. MAG and MAL showed a tendency for upregulation in some of the NAWM cases, whereas PLP and CNP were mostly unaltered. In contrast, MS2 showed a downregulation of all the myelin genes analyzed, indicating that this case might be affected by an oligodendrogliopathy.

A major feature of MS is inflammatory cell infiltration. Microarray studies of demyelinating lesions showed a whole pattern of changes in inflammatory mediator genes (24). In contrast, in our study an overall analysis of inflammation related genes did not show significant alterations in NAWM of MS patients (data not shown). The expression patterns of pro-inflammatory markers such as cytokines (eg, TNFα, interleukins, IFNγ), chemokines and complement factors were not generally altered, which correlated well with our immunohistochemistry data showing that T-lymphocytes were scant or absent. In contrast, we found that activated macrophages/microglia were present throughout the NAWM tissues in all MS cases (Figure 1G). This finding correlates well with the increased levels of the transcription factor STAT6 in all MS cases (Table 2, Cluster I) and the chemoattractant cytokine endothelial-monocyte activating polypeptide II (EMAPII, Table 2, Cluster IIB). High levels of STAT6 in all MS cases may suggest that there is a persistent activation of macrophages/microglia in MS.

Astrogliosis has been described to be a prominent feature in NAWM in MS (2). Although reactive astrocytes are depicted nearby demyelinating lesions, it is not a general phenomenon throughout the NAWM, as demonstrated by quantitative RT-PCR analysis of GFAP (Figure 3A) and confirmed by immunohistochemistry. Nevertheless, significant upregulation of TGFβ2 and the taurine transporter in all MS cases suggests that some changes in transcriptional regulation in astrocytes occurred.

Since many of the genes found to be differentially expressed in our study are known to be expressed in neurons, we investigated the neuronal content in subcortical white matter tissues. RT-PCR for NSE demonstrated the presence of neurons in the subcortical white matter, and in controls NSE mRNA levels were comparable throughout the different cortical regions (Figure 3C). However, much higher expression levels for NSE were detected in NAWM of all MS cases (Figure 3A, C). In situ hybridization of cortical brain tissues showed strong expression of NSE (Figure 4A, B), Snap25 (Figure 4C, D) and GAP43 (not shown) in layer VI neurons as well as in the sub-cortical white matter (arrows). Immunohistochemistry for GFAP (Figure 4G), PLP and MOG (not shown) showed no colocalization with astrocytes or oligodendrocytes. Quantification did not reveal a difference in the total number of neurons in NAWM of the MS cases (data not shown), indicating higher expression levels of NSE mRNA in neurons from NAWM of MS patients. Upregulation of neuronal genes was not a general feature since GAP43 expression for example was not significantly altered (Table 2, Cluster IIC). In situ hybridization for PLP showed a

Cluster 1		MEDIAN of ratios against all controls										*p*-value
gene bank accession	gene name	MS26	MS1 A3B2	MS12 P1A4	MS5 A3C2	MS3 A4B4	MS1 A3D1	MS2 P5C4	MS5 A3C7	MS20 P3B3	MS10 A4D3	MS18 P3B4	
L05500	adenylate cyclase type I	1.9	11.5	2.8	13.7	7.5	9.4	6.7	0.9	1.6	2.6	0.7	0.0132
D00099	sodium/potassium-transporting ATPase alpha 1 subunit	1.3	3.2	3.2	2.7	4.8	5.7	3.2	1.2	1.9	1.6	1.6	0.0009
M65066	cAMP-dependent protein kinase type I beta regulatory subunit	2.6	3.2	1.9	2.2	5.9	7.7	3.4	1.4	1.4	1.7	1.0	0.0034
Y09689	neurogranin (NRGN) *	2.6	3.3	2.2	2.4	5.2	4.8	3.0	1.2	1.8	2.0	1.1	0.0026
AF056085	GABA-B receptor 2 subunit (GABA-BR2)	6.3	5.9	2.8	2.6	16.1	19.1	5.6	1.8	0.9	3.3	0.8	0.0082
L19761	synaptosomal-associated protein 25 (SNAP-25) *	5.4	9.4	5.5	6.2	13.3	12.7	6.3	2.9	0.9	4.4	1.5	0.0016
L20422	14-3-3n protein eta	4.1	2.7	2.7	4.0	4.9	5.3	3.2	2.3	1.0	2.1	0.8	0.0055
M92381	thymosin beta-10	2.0	1.3	1.4	1.6	2.1	2.6	2.2	1.6	1.2	1.4	0.8	0.0012
Y15065	voltage-gated potassium channel	3.6	1.5	2.1	2.1	6.7	5.4	7.0	1.0	0.8	1.5	0.4	0.0693
L14778	calmodulin-dependent calcineurin A subunit alpha isoform	1.7	1.6	2.2	2.5	5.6	6.4	3.6	1.2	1.0	1.4	0.3	0.0109
X06389	synaptophysin (SYP)	2.4	2.0	0.6	2.3	7.1	9.1	2.0	1.6	0.9	2.1	0.7	0.0986
X15376	GABA(A) receptor gamma-2 subunit precursor	0.3	8.6	2.3	3.5	11.6	10.6	3.5	1.9	0.7	1.5	0.6	0.0986
M81883	glutamate decarboxylase 67-kDa isoform (GAD-67)	1.7	3.1	3.2	1.3	7.5	13.8	2.3	2.6	0.4	1.5	1.8	0.0575
U07236	proto-oncogene tyrosine-protein kinase lck	3.3	2.1	2.7	2.0	2.2	1.5	3.3	1.2	1.4	1.6	0.8	0.0132
M25756	secretogranin II precursor; chromogranin C	2.4	2.5	2.3	2.7	5.1	4.1	1.9	3.6	0.9	1.8	0.9	0.0208
S75989	sodium- & chloride-dependent GABA transporter 3	4.7	3.6	2.5	3.9	5.1	3.9	2.7	0.4	1.0	1.4	1.6	0.0829
U61166	SH3P17 SH3 domain-containing protein	3.0	2.2	2.4	2.2	2.5	3.1	3.2	1.5	1.5	1.8	0.7	0.0082
M23619	high mobility group protein (HMG-I)	1.5	1.2	1.8	1.6	2.2	2.5	1.9	1.1	1.3	1.3	0.8	0.0693
X66533	guanylate cyclase soluble beta-1 subunit	2.2	2.5	1.7	2.2	4.4	3.7	2.1	1.1	0.8	1.3	0.7	0.0168
L36151	phosphatidylinositol 4-kinase alpha	2.6	2.8	2.1	2.4	4.9	5.1	2.2	1.6	1.4	1.3	1.4	0.0030
U14722	activin type I receptor	1.9	2.9	2.3	2.3	3.0	3.4	1.5	1.2	1.0	1.0	0.7	0.0390
U24152	p21-activated kinase alpha (PAK1)	2.5	5.7	2.4	2.3	4.6	7.9	2.2	2.4	1.1	1.3	1.7	0.0132
D84476	MAP/ERK kinase kinase 5; MAPKKK5; MEKK5	2.6	2.6	2.2	1.8	2.4	2.7	2.2	1.1	1.4	1.1	0.7	0.0258
J05252	neuroendocrine convertase 2 precursor (NEC 2)	1.0	2.6	1.4	1.8	3.1	6.2	1.9	1.8	0.9	1.3	0.1	0.0475
L24959	Ca^{2+}/calmodulin-dependent protein kinase type IV catalytic subunit	1.6	3.5	1.1	1.5	3.7	6.5	1.8	1.3	0.8	0.9	0.3	0.0693
U07139	dihydropyridine-sensitive L-type calcium channel beta-3 subunit	3.0	5.7	1.8	2.4	2.8	4.3	3.0	0.7	0.7	2.3	0.3	0.0693
D28538	metabotropic glutamate receptor 5 precursor (MGLUR5)	4.9	5.0	2.8	1.8	4.5	6.8	3.2	2.0	0.8	0.6	0.2	0.0575
M88461	neuropeptide Y receptor type 1 (NPY1R)	3.1	3.5	1.6	1.4	2.9	3.1	1.2	1.0	0.6	1.1	0.5	0.0986
M31630	cAMP response element binding protein (CRE-BP1); ATF2	1.6	2.8	1.8	2.0	2.4	1.5	2.4	1.2	1.1	1.1	0.5	0.0390
M32865	Ku 70-kDa subunit; ATP-dependent DNA helicase II	2.9	3.5	1.4	1.2	3.4	2.7	1.2	1.9	0.6	1.2	0.7	0.0208
L36870	c-jun N-terminal kinase kinase 1 (JNKK); MAP kinase kinase 4	2.8	2.2	1.6	0.8	3.4	2.2	1.4	1.4	0.7	0.8	0.3	0.2477
M30773	calcineurin B subunit isoform 1	3.3	3.8	1.1	1.9	6.2	5.0	5.3	1.9	1.7	1.7	0.5	0.0105
U69883	calcium-activated potassium channel HSK1	4.1	4.4	2.0	1.4	5.4	6.2	4.6	2.2	0.7	1.8	0.4	0.0208
U18087	3'5'-cAMP phosphodiesterase HPDE4A6	1.3	5.9	1.2	1.8	3.7	3.9	3.4	1.3	1.0	1.5	0.6	0.0208
U92436	putative protein-tyrosine phosphatase PTEN	1.8	4.0	1.3	1.5	2.3	3.0	2.4	1.2	1.1	1.1	0.6	0.0475
U07819	contactin precursor (CNTN1); glycoprotein gp135	2.3	2.9	2.0	1.4	3.2	4.5	2.1	1.0	1.6	0.9	0.6	0.0575
J04102	C-ets-2	2.9	3.4	2.5	1.8	3.7	4.0	2.0	1.7	1.8	0.5	1.3	0.0105
Y07701	puromycin-sensitive aminopeptidase (PSA)	2.1	2.9	1.8	1.5	1.9	2.1	1.6	1.2	1.5	0.9	1.1	0.0039
AF051334	nibrin (NBS1)	3.3	5.0	1.0	1.7	3.2	1.6	2.5	1.7	2.1	1.2	1.0	0.0082
M28210	ras-related protein RAB3A	5.5	8.2	2.7	3.5	8.0	13.2	2.9	2.0	1.5	1.5	1.6	0.0016
L20977	plasma membrane calcium-transporting ATPase isoform 2	5.4	4.9	2.4	3.0	8.6	12.5	5.8	2.2	0.9	2.7	0.7	0.0043
U50358	Ca^{2+}/calmodulin-dependent protein kinase type II beta subunit	4.9	5.8	4.3	5.2	8.6	11.5	4.3	2.4	1.4	2.0	1.8	0.0034
M27545	protein kinase C beta I (PKC-beta-1)	3.1	3.5	2.4	2.1	6.7	6.9	2.4	1.5	1.0	1.5	0.7	0.0055
L02752	voltage-gated potassium channel protein KV12; HUKIV; HBK5	5.5	4.6	3.3	2.2	10.1	10.3	5.6	2.0	1.4	1.7	0.4	0.0082
M64752	glutamate receptor 1 precursor (GLUR-1); ampa1	4.1	5.5	2.9	2.2	6.6	6.2	3.5	1.9	1.1	1.4	0.5	0.0073
M62843	paraneoplastic encephalomyelitis antigen HUD; HU-antigen D	6.4	5.6	5.2	1.8	12.9	11.2	3.1	1.4	0.8	2.7	0.5	0.0258
U90278	N-methyl D-aspartate receptor subtype 2B (NMDAR2B; NR2B)	4.8	4.5	2.3	2.2	3.3	8.5	3.7	1.5	0.6	1.6	0.7	0.0575
M95585	hepatic leukemia factor (HLF)	3.1	4.6	1.8	2.7	5.4	7.1	3.8	1.8	0.9	1.5	0.4	0.0693
U83192	presynaptic density protein 95 (PSD95); DLG4	2.2	1.9	0.7	1.3	3.7	4.4	1.2	1.6	0.6	1.0	0.5	0.0390
U25265	MAP kinase kinase 5; MAPKK 5	1.8	2.0	1.6	1.3	2.9	2.4	0.9	1.6	1.2	1.0	0.9	0.0475
X07767	cAMP-dependent protein kinase alpha-catalytic subunit	1.9	3.0	1.5	1.8	3.2	4.1	1.3	1.0	1.5	0.7	1.0	0.0449
X66363	serine/threonine-protein kinase PCTAIRE 1 (PCTK1)	3.2	3.6	2.0	1.8	3.0	4.3	1.2	1.5	1.5	0.8	1.8	0.0166
U67733	cGMP-dependent 3',5'-cyclic phosphodiesterase (CGS-PDE)	2.8	4.3	2.6	1.8	6.2	7.6	4.7	0.8	1.8	2.2	0.7	0.0208
L49207	focal adhesion kinase 2 (FADK2; FAK2)	1.8	4.7	2.0	1.8	4.4	7.5	2.4	1.3	1.0	1.5	0.8	0.0318
M24898	triiodothyronine receptor; thyroid hormone receptor (THRA1)	2.8	4.1	2.1	3.2	5.1	8.0	4.7	1.1	0.8	1.4	1.5	0.0055
L33801	glycogen synthase kinase 3 beta (GSK3 beta)	3.1	2.5	1.7	1.8	3.2	3.3	2.1	1.1	1.2	1.1	1.1	0.0039
X76104	death-associated protein kinase 1 (DAP kinase 1; DAPK1)	5.0	3.6	2.5	2.6	4.7	5.4	3.3	2.4	1.7	1.4	1.4	0.0039
Y11044	GABA-B receptor 1A subunit (GABA-BR1A)	4.5	2.2	2.4	1.3	3.9	4.2	2.4	1.2	1.9	1.7	1.1	0.0087
M60119	human immunodeficiency virus type I enhancer-binding protein 2	2.5	1.8	1.5	1.9	4.0	6.0	3.6	1.4	1.5	1.1	1.1	0.0105
U07616	amphiphysin (AMPH)	4.9	7.2	4.2	3.6	12.0	13.4	4.3	2.5	0.7	1.4	0.6	0.0390
M81768	sodium/hydrogen exchanger 1 (Na+/H+ exchanger 1; NHE1)	2.3	3.4	2.6	1.2	3.8	4.5	3.3	1.6	1.3	1.7	1.0	0.0132
M88163	global transcription activator SNF2L1	2.4	2.7	3.1	1.0	2.1	4.0	2.5	1.8	1.2	0.7	0.8	0.0986
M25269	elk-1; ets-related proto-oncogene	2.3	3.4	1.6	1.2	3.0	3.4	2.7	1.3	1.2	0.4	0.4	0.1864
L20814	glutamate receptor 2 precursor (GLUR2)	2.2	3.8	2.3	1.3	4.4	3.0	1.6	1.4	1.1	0.7	0.5	0.1604
AF051782	diaphanous 1 (HDIA1)	2.9	5.5	3.1	1.2	3.1	2.7	3.2	1.9	1.2	1.0	1.0	0.0390
M73238	ciliary neurotropic factor receptor (CNTFR)	2.4	3.3	1.3	1.5	2.6	2.4	1.7	1.3	1.4	0.6	1.1	0.1052
X82260	ran GTPase activating protein 1 (RANGAP1)	1.2	1.1	2.2	1.8	1.9	2.5	2.9	0.9	0.7	1.6	1.5	0.0206
X12795	v-erbA related protein (EAR3)	1.5	1.1	2.1	1.4	2.9	3.0	3.5	0.7	1.3	1.4	1.0	0.0308
J04111	c-jun proto-oncogene; transcription factor AP-1	1.4	1.8	1.9	1.2	1.8	3.0	3.2	0.6	1.0	1.2	1.2	0.0641
M64930	protein phosphatase PP2A 55-kDa regulatory subunit	0.5	1.6	1.6	1.8	2.2	2.0	2.0	1.0	0.9	1.0	0.7	0.2801
X59932	c-src kinase (CSK)	1.0	1.6	1.8	1.9	1.9	1.9	1.3	1.5	0.7	1.3	0.8	0.1167
X94991	zyxin + zyxin-2	2.8	1.9	2.3	1.8	7.7	3.8	2.1	1.2	1.9	1.0	1.7	0.0132
U24497	polycystin precursor	2.2	1.4	2.3	1.3	4.5	2.3	2.9	1.8	2.1	1.0	1.3	0.0168
L14595	neutral amino acid transporter A (SATT)	2.6	1.5	1.4	1.7	3.6	3.9	2.2	0.7	0.9	1.3	1.2	0.1167
AF077866	E16 amino acid transporter	2.1	2.1	1.6	2.1	3.4	1.9	1.9	1.1	1.4	1.0	1.5	0.0390
M20681	brain glucose transporter 3 (GTR3)	2.2	1.8	3.2	1.6	4.1	2.9	2.5	1.3	1.8	0.9	2.6	0.0208
Z18956	sodium- & chloride-dependent taurine transporter	2.1	1.8	3.6	5.3	3.1	3.5	2.8	2.0	2.1	2.5	2.9	0.0258
U16031	signal transducer and activator of transcription 6 (STAT6)	2.8	3.8	2.8	3.0	3.1	2.9	4.5	1.9	1.5	1.5	2.0	0.0050
V00568	c-myc oncogene	2.2	3.6	2.3	1.4	1.3	2.3	3.3	1.1	1.5	1.3	2.0	0.0043
L22075	guanine nucleotide regulatory protein alpha-13 subunit; G13	1.7	2.4	2.2	1.8	1.7	1.9	2.0	1.2	1.9	0.7	1.8	0.0258
U17032	GAP-associated protein	2.2	2.1	2.0	1.6	1.5	1.3	2.2	1.4	1.6	1.0	1.1	0.0043
U12140	TRKB tyrosine kinase receptor *	2.1	2.6	1.5	1.9	2.4	2.9	1.4	1.7	1.0	0.7	1.3	0.0760
M19154	transforming growth factor beta2 precursor (TGF-beta2; TGFB2)	2.5	3.1	1.5	3.0	2.3	1.8	1.7	2.2	0.9	1.0	2.6	0.0087
X12646	serine/threonine protein phosphatase PP2A-alpha subunit	0.9	2.3	1.3	1.0	3.2	3.0	2.2	1.0	1.7	1.0	1.2	0.0372
X65293	protein kinase C epsilon type (NPKC-epsilon)	2.2	2.1	1.8	0.7	6.9	6.7	3.6	1.1	1.5	1.2	1.0	0.0475
U40343	cyclin-dependent kinase 4 inhibitor D (CDKN2D); p19-INK4D	1.8	2.4	2.1	0.6	2.2	3.3	1.3	0.4	1.3	1.2	1.2	0.0372
M24398	parathymosin	2.8	2.1	1.1	1.5	3.5	3.8	1.9	1.2	2.0	1.3	2.0	0.0136
Z81326	neuroserpin precursor; protease inhibitor 12	2.1	4.2	2.9	1.0	3.1	2.6	2.9	1.2	3.9	1.3	0.8	0.0082
M35663	interferon-inducible RNA-dependent protein kinase (P68 kinase)	3.2	4.6	1.3	1.5	2.3	2.4	2.2	1.0	1.8	0.9	1.8	0.0050
X52541	early growth response protein 1 (hEGR1); KROX24	4.4	15.0	2.2	2.1	2.5	3.6	3.2	1.7	1.9	1.8	1.4	0.0055
X59738	zinc finger X-chromosomal protein (ZFX)	2.7	2.1	2.8	1.8	1.7	2.5	2.0	0.6	2.5	1.3	2.1	0.0253
L08807	protein-tyrosine phosphatase 2C (PTP-2C); SH-PTP2	1.6	1.9	2.3	1.6	1.6	1.9	2.0	1.0	2.1	1.3	1.4	0.0136
U59747	apoptosis regulator bclw; BCL2L2	3.5	2.8	1.5	1.4	2.9	1.7	2.6	0.9	3.4	1.2	1.0	0.0208
U08316	ribosomal S6 kinase 2 (RSK2)	2.3	2.2	3.5	1.2	2.1	2.0	1.6	1.0	1.7	1.7	1.7	0.0166
X75621	tuberin; tuberous sclerosis 2 protein (TSC2)	2.3	2.0	2.2	1.1	1.5	2.2	2.1	0.9	1.9	1.3	1.5	0.0206

M29645	insulin-like growth factor II (IGF2)	3.4	1.7	1.7	0.9	2.1	2.7	0.9	0.8	1.8	1.3	0.6	0.0693
M91815	cell division cycle protein 25 nucleotide exchange factor (CDC25)	2.1	1.5	1.0	0.7	3.3	4.4	2.1	0.6	2.1	0.8	1.4	0.0986
U04811	trophinin	3.1	1.1	2.8	1.7	2.9	3.1	1.8	1.1	2.0	1.6	0.8	0.0390
U08839	urokinase-type plasminogen activator receptor precursor	2.9	0.8	2.1	1.3	2.3	1.6	1.9	1.1	1.7	1.4	0.9	0.0390
U03494	transcription factor LSF	2.0	1.6	2.0	1.4	1.8	2.0	0.7	1.1	1.9	1.3	0.5	0.1167

Cluster 2 A		MEDIAN of ratios against all controls											*p*-values
gene bank accession	gene name	MS26	MS1 A3B2	MS12 P1A4	MS5 A3C2	MS3 A4B4	MS1 A3D1	MS2 P5C4	MS5 A3C7	MS20 P3B3	MS10 A4D3	MS18 P3B4	
L34060	cadherin 8 (CDH8)	1.7	2.8	2.7	1.7	3.0	3.8	1.5	1.0	1.5	0.7	0.9	0.0390
U07707	epidermal growth factor receptor substrate 15 (EPS15)	1.7	1.7	1.8	1.4	2.1	3.1	1.4	1.2	1.6	0.8	1.8	0.0206
X79389	glutathione S-transferase theta 1 (GSTT1)	2.2	3.2	1.8	1.5	1.3	1.9	1.8	1.3	1.1	1.0	0.6	0.0372
M97190	Sp2 protein	1.7	2.1	1.9	1.7	1.7	1.6	1.1	1.1	1.7	0.9	1.3	0.0136
D00759	proteasome component C2; macropain subunit C2	1.6	2.8	1.9	1.5	2.0	2.8	1.7	1.2	1.2	0.9	1.1	0.0087
U58198	interleukin enhancer-binding factor (ILF)	1.8	2.5	1.5	1.4	2.5	2.5	1.5	1.2	1.7	0.5	1.0	0.0166
U22431	hypoxia-inducible factor 1 alpha (HIF1 alpha)	1.5	6.5	2.3	2.2	2.0	3.6	1.0	1.8	2.3	0.5	1.4	0.0168
S40706	growth arrest & DNA-damage-inducible protein 153 (GADD153)	3.4	2.8	2.8	2.7	1.9	1.9	2.1	2.4	1.8	1.3	1.8	0.0012
AF060515	cyclin K	1.9	2.4	1.9	1.6	1.6	1.2	1.3	0.9	1.5	0.8	1.8	0.0168
U13897	synapse-associated protein 97 (SAP97)	1.8	2.7	1.3	1.4	2.0	1.6	1.2	1.2	2.8	1.2	1.3	0.0132
U09564	serine kinase	2.1	3.5	2.7	1.4	1.8	2.9	1.4	1.2	1.4	1.2	0.9	0.0258
L13738	tyrosine-protein kinase ack	3.4	7.7	2.3	1.7	2.3	1.9	1.7	1.3	1.4	1.1	1.2	0.0026
M76541	transcriptional repressor protein yin & yang 1 (YY1)	2.5	11.3	2.8	1.5	1.8	1.7	1.2	1.0	1.5	1.1	1.2	0.0258
M86492	glia maturation factor beta (GMF-beta)	1.8	3.9	1.7	1.7	1.0	1.5	0.8	1.4	1.6	1.4	0.8	0.0168
Y00757	neuroendocrine protein 7B2 precursor; secretogranin V	2.0	1.1	1.6	1.7	2.2	2.9	1.4	1.2	1.1	1.6	1.3	0.0206
K03515	neuroleukin (NLK); glucose-6-phosphate isomerase (GPI)	2.7	1.0	2.2	2.5	2.8	3.6	2.0	1.6	1.3	1.6	0.9	0.0043
X57346	14-3-3 protein beta/alpha	1.0	1.6	2.2	2.5	2.8	2.4	1.7	1.7	1.7	1.2	1.4	0.0014
D26309	LIM domain kinase 1 (LIMK-1)	4.4	4.0	3.8	3.0	3.0	5.1	3.7	1.7	1.2	2.0	1.2	0.0017
M90813	G1/S-specific cyclin D2	6.6	3.2	2.9	2.5	4.2	5.0	2.6	2.3	1.4	2.0	0.7	0.0030
X16706	fos-related antigen 2 (FRA2)	4.4	4.2	1.6	1.9	2.7	3.9	3.0	2.3	0.7	1.0	2.4	0.0082
M28213	ras-related protein RAB2	1.6	2.3	1.5	1.3	1.9	2.1	1.2	1.3	1.1	0.8	1.2	0.0055
M35203	Janus kinase 1 (JAK1)	1.5	4.3	1.7	1.9	2.1	2.6	1.9	1.4	1.4	0.9	1.3	0.0050
X14767	GABA(A) receptor beta-1 subunit precursor	5.6	5.0	2.6	2.1	3.7	3.8	2.4	2.0	1.3	0.6	0.8	0.0390
U34819	C-jun N-terminal kinase 3 alpha2 (JNK3A2)	3.7	5.4	3.4	1.8	3.2	4.9	3.0	1.8	1.0	0.7	0.9	0.0166
D26155	transcriptional activator hSNF2-alpha	3.0	2.3	2.9	2.2	2.4	2.8	2.1	1.6	1.6	1.0	0.8	0.0087
AF002999	TTAGGG repeat binding factor 2 (hTRF2)	2.3	2.9	2.0	1.7	2.5	2.4	1.3	1.2	1.1	0.8	0.8	0.0575
X15219	snoN oncogene	2.2	4.6	2.6	2.0	2.2	2.7	1.8	1.4	1.4	1.4	0.8	0.0208
L41816	Ca^{2+}/calmodulin-dependent protein kinase I (CAMKI)	3.3	5.8	3.0	2.3	3.3	3.5	1.5	2.2	0.9	0.8	0.7	0.0258
U00115	B-cell lymphoma 6 protein (bcl-6)	4.1	6.4	3.1	3.3	1.9	2.3	2.2	2.5	0.9	0.7	1.6	0.0206
M96684	purine-rich single-stranded DNA-binding protein alpha (PURA)	2.7	2.9	2.5	1.9	1.3	1.6	2.2	1.6	1.1	1.0	1.4	0.0449
X02811	platelet-derived growth factor B subunit precursor (PDGFB)	6.8	7.9	2.4	2.9	2.7	2.8	1.9	2.3	1.2	0.9	0.8	0.0105
M97287	special AT-rich sequence binding protein 1 (SATB1)	3.6	8.5	2.3	2.8	2.4	2.1	2.5	2.1	1.5	0.9	1.1	0.0055
J03250	DNA topoisomerase I (TOP1)	3.6	4.2	2.8	2.3	2.4	2.0	1.8	2.3	1.6	1.0	1.3	0.0064
D21090	xeroderma pigmentosum group C repair complementing protein	2.6	2.6	2.1	2.0	1.9	1.3	1.7	1.7	1.1	1.0	1.1	0.0166
M31145	insulin-like growth factor binding protein 1 (IGFBP1)	2.4	3.0	2.0	2.2	1.8	1.4	1.3	2.0	1.3	1.1	1.1	0.0069
L11672	zinc finger protein 91 (ZNF92); HPF7; HTF10	3.2	4.7	2.5	3.0	2.9	2.6	1.8	2.2	1.7	1.0	1.1	0.0034
M29870	p21-rac1	2.0	3.1	1.5	1.8	1.7	1.5	1.3	1.5	1.9	1.1	1.1	0.0034
Y00815	leukocyte antigen-related protein precursor (LAR)	1.6	2.9	1.9	2.2	2.2	1.8	1.6	1.7	1.8	1.1	0.8	0.0109
M73077	glucocorticoid receptor repression factor 1	4.3	2.0	0.4	1.9	2.1	2.3	1.9	1.7	1.6	1.5	0.8	0.0168
M74088	adenomatous polyposis coli protein (APC protein)	4.2	3.1	2.9	3.3	4.1	3.6	2.9	3.3	2.0	1.1	1.9	0.0069
L29511	SH2/SH3 adaptor GRB2	2.2	2.1	2.0	2.7	2.0	2.5	1.4	2.2	1.4	1.1	0.9	0.0136
U44378	mothers against dpp homolog 4 (SMAD4)	1.9	1.7	1.5	1.5	1.7	1.6	1.4	2.4	1.4	0.9	1.2	0.0030
U25435	transcriptional repressor CTCF	2.4	1.2	2.3	2.5	2.2	2.6	1.2	1.8	1.0	1.2	0.9	0.0986
D31840	atrophin-1	2.7	1.6	1.8	2.0	3.7	4.0	1.0	0.7	0.6	1.2	1.2	0.1372
X15218	ski oncogene	2.7	2.6	3.0	2.9	2.6	3.4	1.6	1.6	1.5	1.2	1.8	0.0069
X86779	Fas-activated serine/threonine (FAST) kinase	2.4	1.6	1.6	1.5	2.1	2.0	1.1	1.2	1.3	1.0	1.2	0.0132
M64788	rap1 GTPase activating protein 1 (RAP1GAP)	5.8	2.3	3.1	3.1	2.6	3.7	2.5	1.6	0.8	1.7	1.0	0.0206
M25627	glutathione S-transferase A1	3.4	1.7	1.9	1.9	1.7	1.8	1.8	1.5	1.1	1.2	1.2	0.0087
M76125	tyrosine-protein kinase receptor UFO precursor; axl oncogene	3.6	2.1	1.5	1.5	2.9	2.1	1.4	1.4	0.9	0.8	1.2	0.0829
M22199	protein kinase C alpha polypeptide (PKC-alpha)	2.0	2.0	1.5	1.7	2.0	3.3	1.4	1.4	1.0	0.9	1.0	0.0308
X01060	transferrin receptor (TFRC)	1.9	2.8	1.7	1.8	2.0	4.3	1.2	1.9	0.8	1.1	1.3	0.0258
L05624	MAP kinase kinase 1; MAPKK 1; MKK1; ERK activator kinase 1	3.7	6.3	2.3	2.1	1.9	4.1	1.6	2.0	0.7	1.3	0.7	0.0132
L31951	c-jun N-terminal kinase 2 (JNK2); JNK55	2.3	3.8	1.9	1.7	1.8	2.6	1.3	1.4	0.7	0.7	0.7	0.0390
L09247	protein-tyrosine phosphatase gamma precursor (R-PTP-gamma)	3.1	2.5	2.7	1.6	1.6	2.4	1.6	1.2	0.7	1.0	0.5	0.1864
X66945	N-sam; fibroblast growth factor receptor1 precursor (FGFR1)	3.7	4.7	2.7	2.8	2.0	2.8	1.8	1.5	1.0	0.9	0.6	0.0693
U35835	DNA-dependent protein kinase (DNA-PK)	3.3	3.3	3.0	2.1	1.7	2.8	1.3	2.0	0.8	0.7	0.9	0.0986
M87503	IFN-alpha responsive transcription factor subunit	2.0	2.0	2.0	1.2	1.7	1.8	1.3	1.4	1.3	0.6	1.5	0.0308
AF082556	TRF1-interacting ankyrin-related ADP-ribose polymerase tankyrase	1.1	2.3	2.3	1.9	1.9	3.1	1.1	1.3	1.8	0.8	1.4	0.0575
M11233	cathepsin D precursor (CTSD)	1.6	1.2	1.9	2.1	1.5	2.1	1.0	1.7	1.0	0.9	1.5	0.1649
K03195	erythrocyte glucose transporter 1 (GLUT1)	1.4	1.0	2.6	1.9	1.2	2.0	1.0	1.3	1.2	1.0	1.3	0.0896
L12579	CCAAT displacement protein; CUTL1; CASP	3.1	1.9	2.0	2.2	1.1	1.7	1.0	1.1	1.5	1.2	1.2	0.1427
X02751	N-ras; transforming p21 protein	3.8	1.8	2.3	2.1	1.0	1.5	0.7	1.1	0.9	1.1	1.1	0.2472
M80629	CDC2-related protein kinase CHED	4.6	3.9	3.2	1.9	2.4	3.0	0.6	0.8	1.7	0.7	2.1	0.1864
S83171	BCL-2 binding athanogene-1 (BAG-1)	1.9	1.6	2.0	1.7	1.5	1.9	0.6	1.3	1.8	1.3	1.0	0.0208
L02750	voltage-gated potassium channel protein KV11; HUKI; HBK1	5.7	3.4	1.3	1.9	3.9	1.4	3.2	1.1	0.8	1.5	0.8	0.0693
L07868	ERBB4 receptor protein-tyrosine kinase	4.1	4.2	2.3	2.3	2.7	2.3	2.8	1.0	1.6	1.1	0.6	0.0829
X12794	v-erbA related protein (EAR2)	2.0	3.3	1.8	1.0	1.7	1.3	2.4	1.0	0.7	0.8	0.6	0.3637
U25278	extracellular signal-regulated kinase 5 (ERK5); BMK1 kinase	3.3	3.4	1.6	1.1	2.2	1.4	1.3	2.0	1.3	0.6	1.4	0.0318
U13021	caspase-2 precursor (CASP2)	4.2	3.8	2.8	1.6	2.0	1.7	1.8	1.5	1.4	0.8	1.2	0.0390
L33264	cdc2-related protein kinase PISSLRE	4.2	2.8	1.9	1.6	2.1	0.9	2.1	1.8	1.4	0.6	1.1	0.1604
M22995	ras-related protein RAP-1A; GTP-binding protein SMG-p21A	8.4	2.2	2.9	2.0	1.8	2.1	2.7	2.0	1.8	0.9	2.0	0.0829
U05040	FUSE binding protein	2.4	2.1	1.4	1.5	1.6	1.8	2.0	1.1	1.6	0.7	1.6	0.1372
M21121	rantes pro-inflammatory cytokine *	3.5	2.9	1.1	1.3	1.0	0.9	2.0	1.5	1.6	0.7	0.7	0.1228
X01057	interleukin-2 receptor alpha subunit precursor	3.6	7.1	2.1	2.7	1.1	1.0	2.9	2.1	1.6	0.6	0.6	0.0538
X03484	c-raf proto-oncogene	3.0	1.7	2.1	1.3	1.4	1.9	1.8	1.1	1.3	1.0	0.6	0.0829
M33336	cAMP-dependent protein kinase I alpha regulatory subunit	1.6	1.4	1.8	1.6	1.8	2.2	1.7	1.3	1.7	1.1	0.7	0.0449
U85245	phosphatidylinositol-4-phosphate 5-kinase II beta	3.1	2.2	2.8	2.2	2.7	3.6	2.4	1.4	1.8	1.2	1.0	0.0206
U16296	T-lymphoma invasion and metastasis inducing TIAM1	3.0	1.9	2.4	1.4	2.6	4.0	1.7	1.2	1.0	0.8	0.6	0.1864
X04434	insulin-like growth factor I receptor (IGF1R)	3.1	1.6	2.4	1.7	1.9	1.8	1.7	1.2	1.1	1.0	0.5	0.1167
Y00285	cation-independent mannose-6-phosphate receptor precursor	3.8	2.4	3.1	1.9	1.9	2.1	1.7	1.6	1.5	1.1	0.5	0.0475
D26156	estrogen receptor hSNF2b	2.3	1.6	2.3	1.1	2.0	1.7	1.4	1.2	1.4	1.1	0.5	0.0575
L20046	xeroderma pigmentosum group G complementing protein (XPG)	2.1	1.8	1.9	0.8	1.8	1.2	1.5	1.2	2.1	1.0	0.6	0.1372
AF045161	cyclin T CDK9-associated	2.6	1.6	1.8	1.1	1.3	1.3	1.5	0.9	1.3	0.7	1.0	0.1604
L14837	tight junction protein zonula occludens (ZO-1)	2.9	3.0	1.9	2.0	1.5	1.4	1.5	0.4	1.3	1.0	0.6	0.2472
M30938	Ku (p70/p80) subunit; ATP-dependent DNA helicase II	3.8	4.6	2.5	1.9	2.1	1.3	1.4	1.0	0.9	0.6	0.6	0.4090
M62831	transcription factor ETR101	3.5	2.3	2.2	2.2	2.1	1.9	2.2	1.9	2.1	1.2	1.0	0.0017
U14417	RalGDSB; RALGEF	1.7	2.2	1.9	1.6	1.6	1.8	2.0	1.2	1.6	0.7	1.2	0.0253
M63488	replication protein A 70-kDa subunit (RPA70; REPA1; RF-A)	2.1	1.9	1.6	2.0	2.0	1.3	1.5	1.2	1.3	0.9	1.2	0.0390
M34667	phospholipase C gamma 1 (PLC-gamma 1; PLCG1)	2.5	1.5	1.8	1.8	1.5	2.4	1.6	1.3	1.3	1.2	1.2	0.0575
L29277	signal transducer and activator of transcription 3 (STAT3)	1.4	2.0	1.7	2.4	1.5	2.0	1.5	1.5	1.0	1.2	1.2	0.0318

X75342	shb proto-oncogene	2.8	1.8	2.3	2.2	1.5	2.2	1.9	1.1	1.3	1.2	1.3	0.0390
U12779	MAP kinase-activated protein kinase 2 (MAPKAPK-2)	2.1	1.7	2.5	2.1	0.7	2.1	1.7	1.1	1.4	1.2	1.6	0.0575
L35253	mitogen-activated protein kinase p38 (MAP kinase p38)	2.2	2.0	2.3	2.0	1.0	1.8	1.4	1.3	1.5	1.0	1.2	0.0641
U08853	transcription factor 11 (TCF11)	2.3	1.9	2.3	1.9	1.6	2.3	1.1	1.7	1.2	1.0	1.1	0.0986
U08191	R kappa B DNA-binding protein	2.5	1.8	1.9	2.2	1.1	2.2	1.2	1.7	1.2	1.1	1.1	0.1228
M81934	CDC25B; CDC25HU2; M-phase inducer phosphatase 2	2.3	1.8	2.1	2.2	1.5	1.6	1.6	1.7	1.7	1.1	0.9	0.0538
M96824	nucleobindin precursor (NUC)	1.8	1.5	1.9	2.1	1.5	1.5	1.3	1.5	1.5	1.3	0.9	0.0449
X06374	platelet-derived growth factor A subunit precursor (PDGFA)	1.7	2.3	1.9	2.0	1.3	1.4	1.0	1.5	1.4	0.9	0.9	0.0641
X79981	vascular endothelial cadherin precursor (VE-cadherin)	1.7	1.6	1.6	1.9	1.2	1.8	0.9	1.3	1.3	0.8	0.8	0.1427
D13866	alpha1 catenin; cadherin-associated protein; alpha E-catenin	1.6	1.8	2.0	2.3	1.3	1.5	1.0	1.8	1.3	1.0	0.6	0.2472
X65778	acidic fibroblast growth factor (AFGF)	2.5	2.1	2.0	2.1	1.0	1.2	0.9	2.1	1.5	1.0	0.6	0.2801
U04847	Ini1	2.7	2.3	2.2	1.6	1.0	1.8	1.0	1.6	1.3	0.7	0.7	0.2170

Cluster 2 B		MEDIAN of ratios against all controls											*p*-values
gene bank accession	gene name	MS26	MS1 A3B2	MS12 P1A4	MS5 A3C2	MS3 A4B4	MS1 A3D1	MS2 P5C4	MS5 A3C7	MS20 P3B3	MS10 A4D3	MS18 P3B4	
K01911	neuropeptide Y precursor (NPY)	2.9	3.7	3.6	3.0	3.0	3.4	0.9	1.9	0.4	1.0	1.5	0.0136
M81882	glutamate decarboxylase 65-kDa isoform (GAD-65)	2.3	4.6	2.9	1.4	4.4	6.4	0.4	1.6	0.7	1.4	0.7	0.1167
X91249	ATP-binding casette 8 (ABC8); Drosophila white homolog	1.9	4.3	1.6	2.2	2.5	1.2	0.4	1.4	1.8	1.5	1.1	0.0208
M97676	MSX-1 homeobox protein; HOX7	2.6	2.9	2.3	2.8	2.3	1.2	2.0	1.6	1.4	1.2	1.4	0.0050
Z23115	apoptosis regulator bcl-x	2.3	1.6	1.9	1.6	1.5	1.2	1.4	1.5	1.8	1.0	1.2	0.0055
D45132	zinc-finger DNA-binding protein	1.7	2.2	2.9	2.9	1.5	0.9	1.4	1.9	1.4	1.3	1.0	0.0253
D28468	albumin D box-binding protein (DBP)	3.0	2.9	2.3	3.3	2.2	1.1	0.9	2.7	1.8	1.0	1.5	0.0449
D28118	putative transcription activator DB1	2.5	2.8	3.0	1.7	1.7	1.4	1.0	1.8	1.7	0.8	1.4	0.0538
M37435	macrophage-specific colony-stimulating factor (CSF-1; MCSF)	3.8	5.6	3.1	2.7	1.9	1.1	1.6	2.4	1.4	1.9	1.0	0.0109
U10117	endothelial-monocyte activating polypeptide II (EMAP II)	3.1	3.1	2.9	1.9	1.4	1.3	1.9	2.2	1.9	1.0	1.1	0.0136
M86400	phospholipase A2	1.4	6.0	2.2	2.9	2.3	1.0	1.0	2.9	0.9	1.5	1.1	0.0475
L31881	nuclear factor I (NFI); NFI-X	2.7	2.2	1.4	1.9	2.3	3.0	1.0	1.6	1.4	0.8	1.1	0.0538
M36340	ADP-ribosylation factor 1	2.4	2.8	1.2	2.1	1.8	2.1	1.0	1.8	1.1	0.8	1.3	0.0372
X85106	ribosomal S6 kinase 3 (RSK3)	2.1	2.7	1.8	1.9	2.2	1.9	0.7	1.6	1.2	0.7	1.0	0.1372
L13616	focal adhesion kinase (FADK)	2.0	2.1	1.7	2.2	1.5	1.6	0.5	1.7	1.3	0.9	1.1	0.2472
X68274	axonin-1 precursor; transient axonal glycoprotein 1 (TAG-1)	1.6	2.2	0.8	2.1	2.3	1.4	0.4	1.5	1.3	0.7	1.9	0.3961
L34075	FKBP-rapamycin associated protein (FRAP)	2.8	4.1	2.5	1.7	2.7	1.4	0.4	1.3	1.1	2.0	0.5	0.0693
M28882	cell surface glycoprotein MUC18	2.7	2.2	1.6	1.3	1.9	1.9	0.6	0.9	0.7	0.7	0.4	0.3159
D00726	ferrochelatase precursor; heme synthetase	2.3	2.0	1.9	1.5	1.7	1.3	0.4	1.1	1.0	0.8	0.4	0.2831
L34673	DNA-binding protein HIP116; ATPase;	1.8	2.4	1.5	1.5	1.2	1.6	0.5	1.1	1.4	0.7	0.6	0.2831
M74524	ubiquitin-conjugating enzyme E2 17-kDa (UBE2A)	1.9	2.2	1.5	1.8	1.8	1.8	0.9	1.6	1.0	0.8	0.8	0.0641
D21235	HHR23A; UV excision repair protein protein RAD23A	1.8	2.3	1.4	1.7	1.5	2.2	0.8	1.5	0.9	0.7	0.7	0.3159
M18112	poly(ADP-ribose) polymerase (PARP);	1.8	2.5	1.7	2.1	1.6	1.8	1.0	1.5	1.5	0.7	0.5	0.0905
M10051	insulin receptor precursor (INSR)	1.4	2.1	2.4	2.0	2.0	1.5	0.8	1.5	1.3	1.0	0.6	0.0693
M84820	retinoic acid receptor beta (RXR-beta)	1.9	2.8	1.5	2.5	1.6	1.8	0.9	1.6	1.2	1.2	0.3	0.1228
M15024	myb proto-oncogene; c-myb	2.1	2.9	2.6	1.8	1.4	2.0	0.9	1.4	1.1	1.4	0.6	0.0829
U13737	caspase-3 (CASP3)	2.1	2.3	2.1	1.6	1.3	2.1	0.6	1.7	1.2	0.8	0.4	0.3637
L05515	cAMP-responsive element-binding protein (CREB1)	2.4	2.7	2.4	2.0	1.3	0.9	0.9	1.6	1.1	0.8	0.6	0.1649
X77722	interferon-alpha/beta receptor beta subunit precursor	1.2	2.4	2.3	2.6	1.1	1.2	0.9	1.5	1.5	0.9	0.8	0.0986
M29366	ERBB-3 receptor protein-tyrosine kinase precursor	1.7	1.8	1.5	1.9	1.4	0.8	0.5	1.5	1.3	0.9	0.9	0.2801
D42108	phospholipase C (PLCL)	1.6	1.7	2.3	1.7	1.1	1.0	0.8	1.3	1.5	0.9	1.0	0.3961
D10924	stromal cell derived factor 1 receptor (SDF1 receptor); CXCR4	1.6	5.9	3.5	2.0	2.7	0.6	0.7	1.7	1.6	2.0	0.9	0.1372
U02687	stem cell tyrosine kinase 1 (STK1)	3.7	4.2	3.7	2.7	0.6	1.9	0.8	1.8	0.9	0.8	0.7	0.1604
X59798	G1/S-specific cyclin D1	2.7	1.9	1.9	2.3	1.0	1.3	0.8	1.5	0.9	1.7	0.8	0.1167
U56390	caspase-9 precursor (CASP9)	1.6	2.2	1.4	0.9	1.1	1.1	1.5	11.6	1.7	1.0	0.4	0.2155

Cluster 2 C		MEDIAN of ratios against all controls											*p*-values
gene bank accession	gene name	MS26	MS1 A3B2	MS12 P1A4	MS5 A3C2	MS3 A4B4	MS1 A3D1	MS2 P5C4	MS5 A3C7	MS20 P3B3	MS10 A4D3	MS18 P3B4	
M61906	phosphatidylinositol 3-kinase regulatory alpha subunit (PI3K)	2.5	3.0	2.0	1.6	1.9	2.3	1.0	1.3	1.7	1.0	1.4	0.0449
M93255	fli-1 oncogene; ergB transcription factor	2.4	3.7	2.8	2.1	1.6	2.1	1.1	1.5	1.7	1.0	0.9	0.0208
X93499	ras-related protein RAB-7	1.5	2.8	1.4	1.5	1.6	2.1	1.1	1.2	1.1	0.5	1.2	0.0449
U12535	epidermal growth factor receptor kinase substrate EPS8	1.8	4.2	2.3	1.7	1.4	2.5	1.3	1.9	0.8	0.8	1.2	0.0829
U43408	tyrosine kinase tnk1	3.3	3.9	2.7	1.9	2.3	2.2	0.9	1.5	0.9	1.0	0.8	0.1167
U10324	nuclear factor NF90	1.4	3.8	1.7	1.3	2.3	2.6	1.2	1.1	1.3	0.5	0.5	0.2477
U63717	osteoclast stimulating factor	0.9	2.5	1.7	1.2	1.9	2.1	1.0	1.7	1.0	0.5	0.7	0.2831
U34846	aquaporin 4; WCH4; mercurial-insensitive water channel	1.6	2.8	0.6	1.4	2.3	1.5	0.9	1.6	1.0	0.4	1.2	0.1649
M15400	retinoblastoma-associated protein (RB1)	1.7	2.5	0.8	1.6	1.6	1.5	1.4	1.7	1.2	0.5	0.8	0.1864
X03124	metalloproteinase inhibitor 1 precursor (TIMP1)	0.8	8.7	1.3	2.3	1.0	2.0	1.4	2.1	0.8	0.5	1.2	0.1864
X57766	matrix metalloproteinase 11 (MMP11); stromelysin 3	1.4	16.9	1.9	4.0	2.1	2.2	1.6	3.1	0.9	0.9	1.5	0.1266
M15800	T-lymphocyte maturation-associated protein MAL	1.1	3.2	1.6	2.0	1.4	1.7	1.0	1.8	1.1	0.7	1.2	0.0760
D10925	CC chemokine receptor type 1 (CCR 1); RANTES receptor	1.1	4.5	1.7	2.0	1.1	1.3	1.2	1.8	0.9	0.6	1.0	0.2170
M21616	platelet-derived growth factor receptor beta subunit (PDGFRB)	3.5	2.6	2.5	1.6	2.9	3.0	1.0	2.0	1.1	1.1	0.6	0.1167
AF052432	katanin p80 subunit	2.5	3.3	1.6	1.5	4.8	5.0	1.5	1.2	1.4	0.5	1.1	0.0693
X00588	epidermal growth factor receptor (EGFR)	2.9	3.7	1.7	1.6	2.9	3.0	3.3	1.0	0.7	0.5	1.7	0.2477
L11353	moesin-ezrin-radixin-like protein (MERLIN); schwannomin (SCH)	3.9	2.9	1.4	2.4	2.9	3.8	2.8	1.6	1.1	0.4	1.0	0.1167
M60915	neurofibromatosis protein type I (NF1); neurofibromin	2.9	3.7	1.5	2.2	2.2	2.5	1.7	1.0	1.5	0.6	0.8	0.1167
U71364	cytoplasmic antiproteinase 3 (CAP3)	2.5	3.5	2.0	1.9	2.2	2.0	1.7	1.9	1.8	0.7	1.3	0.0082
X56681	jun-D	2.1	2.4	0.7	1.6	2.5	2.0	0.8	0.9	1.0	0.7	1.3	0.2472
M25667	neuromodulin; axonal membrane protein GAP-43	2.1	4.2	0.9	1.7	3.7	4.2	1.2	1.2	0.6	1.7	0.6	0.2155
M58051	fibroblast growth factor receptor 3 precursor (FGFR3)	4.5	2.7	0.5	1.7	2.1	2.1	1.7	1.6	0.8	0.9	1.2	0.1167
S40832	early growth response protein 3 (EGR3)	7.4	10.1	1.0	2.7	3.5	0.9	1.2	3.9	0.2	0.3	0.4	0.2477
X59764	DNA-(apurinic or apyrimidinic site) lyase; REF-1 protein	2.2	3.7	1.8	1.9	2.8	1.4	1.1	1.6	0.6	1.1	1.6	0.0475
M97191	Sp3 protein	1.9	3.3	1.7	1.6	1.6	2.0	1.1	2.0	1.1	0.9	0.9	0.0318
M28212	ras-related protein RAB6	2.3	3.9	1.9	2.1	2.2	3.2	1.2	1.5	0.9	0.6	0.9	0.0641
M84489	MAP kinase 2; MAPK 2; p42-MAPK; ERK2	3.1	2.8	2.3	2.5	3.5	3.1	1.1	2.2	1.3	0.9	1.4	0.0206
M68840	monoamine oxidase (MAO-A)	1.9	4.3	2.6	2.8	3.3	2.7	1.7	2.5	1.3	1.2	1.4	0.0475
M92843	tristetraproline (TTP)	3.5	3.7	2.6	4.0	1.7	3.9	2.2	3.1	1.8	1.1	2.4	0.0253
M57230	interleukin-6 receptor beta subunit precursor; gp130	2.1	3.2	1.6	2.7	1.5	2.1	1.1	1.9	1.5	0.9	1.8	0.1052
X68676	glutathione S-transferase mu1 (GSTM1; GST1)	3.1	3.4	1.7	3.1	1.4	2.2	1.5	2.1	1.1	0.9	1.9	0.0308
K02770	interleukin-1 beta precursor (IL1B)	2.6	2.6	1.5	2.2	1.6	1.7	1.2	1.9	0.9	0.8	1.5	0.1228
D14533	xeroderma pigmentosum group A complementing protein	4.4	6.3	2.5	3.7	1.6	2.6	1.6	2.8	1.2	0.6	1.9	0.0986
J03133	transcription factor Sp1 (TSFP1)	0.8	2.1	2.6	2.2	1.6	2.6	1.1	1.9	1.3	0.8	1.1	0.1372
X54637	tyk2 non-receptor protein tyrosine kinase	1.8	2.4	1.4	1.7	2.3	1.8	1.0	1.4	0.8	0.8	1.0	0.3218
M97252	Kallmann syndrome protein precursor (KAL)	2.5	2.0	0.8	1.9	1.8	1.8	0.7	1.6	0.5	1.0	0.6	0.2831
X74794	MCM4 DNA replication licensing factor; CDC21 homolog	3.5	3.4	1.5	2.6	1.6	2.6	1.1	3.1	0.4	1.1	0.3	0.4090
X53587	integrin beta 4	2.8	2.5	1.9	2.3	2.0	1.4	0.9	1.7	0.8	0.9	1.2	0.1427
M96944	paired box protein PAX-5; B-cell specific transcription factor	2.1	2.2	2.1	2.1	1.7	1.5	0.9	1.6	1.2	0.8	0.8	0.1897
L27211	cyclin-dependent kinase 4 inhibitor (CDK4I); p16-INK4	4.5	4.5	3.1	3.4	1.8	1.5	1.1	2.1	1.1	0.8	0.9	0.1167
M23254	calpain 2 large (catalytic) subunit	2.4	1.5	1.9	1.8	1.5	1.4	1.2	1.8	1.1	1.2	1.0	0.1228
X66365	cell division protein kinase 6 (CDK6)	3.4	2.9	2.3	0.9	1.2	2.2	1.2	2.2	0.9	0.8	0.6	0.2155

X13403	octamer-binding transcription factor 1 (oct-1; OTF1)	3.1	3.6	3.1	1.4	2.1	2.4	1.6	1.7	0.9	0.8	0.6	0.1731
M21535	ets-related gene transforming protein (ERG1)	3.8	4.3	2.5	1.4	1.7	1.5	0.8	2.0	1.0	0.9	0.9	0.2155
L29220	CDC-like kinase 3 (CLK3)	1.8	2.5	2.3	1.5	1.3	1.7	1.2	1.9	1.2	0.6	1.0	0.2477
M86546	homeobox protein pbx1; Homeobox protein prl	2.0	2.7	2.3	1.8	1.9	2.4	1.1	2.0	1.0	1.0	0.7	0.0475
M31899	xeroderma pigmentosum group B complementing protein (XPB)	2.4	2.2	2.1	1.4	1.7	1.7	1.3	1.4	1.1	1.1	0.5	0.0693
U22456	5'-AMP-activated protein kinase catalytic alpha-1 subunit	1.5	2.9	2.0	1.8	2.1	2.2	0.8	1.9	1.0	0.7	0.5	0.0829
S75313	Machado-Joseph disease protein 1 (MJD1)	2.1	2.4	2.0	1.6	2.0	1.8	0.7	1.5	0.7	0.8	0.7	0.1167
D26121	ZFM1 protein alternatively spliced product	1.8	2.6	2.3	2.2	1.6	1.7	0.9	1.6	1.1	0.8	0.6	0.1649
L06895	MAD protein; MAX dimerizer	2.7	3.8	2.2	1.5	1.3	2.4	1.8	1.1	0.6	1.0	0.7	0.1864
AF005216	Janus kinase 2 (JAK2); receptor-associated tyrosine kinase	3.0	2.7	2.0	1.2	1.0	2.2	1.3	1.6	1.2	1.5	0.9	0.1864
AF055581	lnk adaptor protein	3.1	3.7	1.9	2.0	1.6	2.5	1.8	1.7	1.5	0.8	1.2	0.0166
AF055377	C-maf transcription factor	4.4	5.2	1.2	2.2	2.1	2.7	2.0	2.6	1.0	0.7	0.8	0.0575
U11732	ets-related protein tel; ets translocation variant 6 (ETV6)	2.7	2.1	1.9	1.8	1.3	2.4	2.5	1.6	0.4	1.1	1.2	0.0132
X05562	procollagen alpha 2(IV) subunit precursor	2.0	4.6	1.0	3.7	2.2	2.2	1.9	2.6	0.5	1.0	0.6	0.1604
M23379	GTPase-activating protein (GAP); p120GAP	1.8	3.2	1.5	1.3	1.4	1.5	1.3	1.9	0.5	1.0	0.6	0.0575
M59818	granulocyte colony stimulating factor receptor (GCSF-R)	3.5	4.5	2.5	3.5	1.2	1.7	1.0	1.9	0.9	0.8	1.2	0.1372
AF078077	growth arrest & DNA-damage-inducible protein 45 beta	4.1	2.8	1.9	2.9	2.0	2.0	1.6	2.1	1.0	1.0	1.4	0.0308
M18391	ephrin type-A receptor 1 precursor	3.0	3.0	2.0	2.8	1.9	2.1	1.4	2.2	1.4	0.9	1.1	0.0449
D88435	cyclin G-associated kinase (GAK)	3.1	2.4	1.6	1.7	2.4	1.5	1.3	1.6	1.3	0.8	1.0	0.0475
X80692	MAP kinase 3 (MAPK3; p97-MAPK); ERK3	2.3	2.8	1.6	2.0	2.3	1.9	1.0	2.2	0.9	0.7	0.5	0.0449
X72304	corticotropin releasing factor receptor 1 precursor	3.1	5.8	2.1	2.5	1.6	1.4	1.4	1.8	1.1	0.8	0.8	0.0986
M33374	NADH-ubiquinone oxidoreductase B18 subunit; complex I-B18	3.1	6.5	2.2	2.6	2.1	1.6	1.4	2.3	1.3	0.7	0.7	0.0372
X54936	placenta growth factors 1 + 2 (PLGF1 + PLGF2)	2.7	4.3	1.7	1.0	1.5	1.2	1.0	1.7	1.5	1.0	1.1	0.2477
S56143	adenosine A1 receptor (ADORA1)	2.2	5.3	2.2	1.8	1.4	1.6	1.3	1.9	1.8	0.7	0.8	0.1228
U28838	transcription factor TFIIIB 90 kDa subunit (HTFIIIB90)	2.1	3.4	1.6	1.2	1.1	1.2	0.7	1.8	1.1	0.9	0.4	0.2650
X87838	beta catenin (CTNNB)	2.2	3.2	1.9	1.7	1.7	1.1	0.8	2.1	1.2	0.8	0.5	0.2472
U33841	ataxia telangiectasia (ATM)	3.2	4.6	2.1	2.0	1.6	0.8	1.6	1.9	1.0	1.1	1.1	0.0693
M87338	replication factor C 40-kDa subunit (RFC40)	2.9	3.8	2.0	2.2	1.6	1.3	1.0	2.2	0.7	1.0	0.8	0.0829
M57627	interleukin-10 precursor (IL-10)	2.4	2.7	1.8	2.0	1.1	1.3	1.3	1.7	1.1	0.8	0.8	0.0449
S59184	related to receptor tyrosine kinase (RYK)	3.0	3.4	2.0	1.9	0.9	1.1	1.1	1.8	0.8	1.1	1.0	0.2155
M73482	neuromedin B receptor (NMBR)	2.4	4.7	1.8	2.2	0.9	1.2	1.0	1.9	0.9	0.9	0.7	0.1897
X53586	integrin alpha 6 precursor (ITGA6); VLA6	2.1	2.2	2.6	1.5	1.5	0.7	1.2	1.5	1.0	0.7	0.5	0.3637
U41766	metalloprotease/disintegrin/cysteine-rich protein precursor	2.6	3.4	1.7	1.9	1.0	1.3	1.4	0.7	0.6	1.2	0.4	0.3218
D49950	interleukin-18 precursor (IL-18)	2.3	2.2	1.2	1.6	1.1	1.5	1.0	1.6	0.6	1.5	0.5	0.2477
X63629	placental cadherin precursor (P-cadherin)	2.7	3.2	2.0	1.8	0.4	2.4	1.3	1.6	0.8	1.0	0.5	0.2477

Cluster 3		MEDIAN of ratios against all controls											*p*-values
gene bank accession	gene name	MS26	MS1 A3B2	MS12 P1A4	MS5 A3C2	MS3 A4B4	MS1 A3D1	MS2 P5C4	MS5 A3C7	MS20 P3B3	MS10 A4D3	MS18 P3B4	
V00530	hypoxanthine-guanine phosphoribosyltransferase (HPRT)	3.7	10.5	0.6	3.1	6.7	4.9	2.8	1.4	1.5	1.0	1.6	0.0258
M93056	leukocyte elastase inhibitor (LEI)	1.9	3.3	1.1	1.7	2.2	1.6	1.1	2.3	1.6	1.0	1.3	0.0986
U09607	janus kinase 3 (JAK3)	3.3	3.4	1.1	1.5	2.0	2.3	6.0	1.5	3.5	0.6	1.3	0.1372
X79067	EGF response factor 1 (ERF1)	2.0	3.0	1.4	1.8	1.5	3.1	2.1	1.4	1.1	0.4	1.7	0.0372
X03663	macrophage colony stimulating factor I receptor (CSF-1-R)	1.9	2.2	1.3	1.8	0.7	3.7	1.7	1.8	0.8	0.5	2.5	0.1167
M24069	DNA-binding protein A	2.3	2.9	2.9	2.5	1.1	2.5	3.0	1.7	0.9	0.5	2.1	0.0372
X02920	alpha-1-antitrypsin precursor	1.1	3.2	3.0	7.6	1.8	2.9	1.3	5.3	0.8	1.2	4.5	0.0693
X76981	adenosine A3 receptor (ADORA3)	2.0	3.8	2.1	3.6	1.1	1.5	0.8	2.5	0.7	1.1	2.2	0.1864
M15395	cell surface adhesion glycoproteins LFA-1/CR3/p150,95 beta	1.7	2.9	2.0	4.2	1.1	1.7	0.7	2.4	0.3	1.1	1.1	0.2831
J03132	intercellular adhesion molecule-1 precursor (ICAM1)	2.2	3.5	1.8	1.9	1.2	2.6	1.9	1.1	1.2	0.7	2.5	0.0475
M60974	growth arrest & DNA-damage-inducible protein (GADD45)	2.5	7.5	2.5	2.8	1.9	5.8	3.9	2.2	0.9	0.4	1.6	0.2170
U09579	cyclin-dependent kinase inhibitor 1; WAF1	3.5	2.5	2.1	1.5	1.4	2.2	2.0	1.6	1.2	0.6	1.6	0.2472
M33294	tumor necrosis factor receptor 1 (TNFR1)	2.8	3.0	1.5	2.3	2.1	1.9	2.1	1.5	1.3	1.2	1.8	0.1604
M24545	monocyte chemotactic protein 1 precursor (MCP1)	3.7	4.6	1.6	1.7	2.2	2.1	6.1	1.9	1.3	0.5	1.4	0.1427
U28014	caspase-4 precursor (CASP4)	2.9	4.1	1.9	1.7	1.4	1.4	2.1	1.9	0.7	0.5	1.3	0.0829
X04366	calpain 1 large (catalytic) subunit	2.7	3.7	1.4	1.8	2.4	2.4	1.9	2.1	0.7	0.6	0.6	0.1167
X74764	neurotrophic tyrosine kinase receptor-related 3; TKT precursor	1.8	2.6	1.8	1.8	1.4	1.9	1.9	1.2	0.8	0.8	1.0	0.0318
K01500	alpha-1-antichymotrypsin precursor (ACT) *	0.8	2.5	1.1	4.0	1.9	1.9	1.9	3.6	0.4	0.5	2.6	0.4875

Cluster 4		MEDIAN of ratios against all controls											*p*-values
gene bank accession	gene name	MS26	MS1 A3B2	MS12 P1A4	MS5 A3C2	MS3 A4B4	MS1 A3D1	MS2 P5C4	MS5 A3C7	MS20 P3B3	MS10 A4D3	MS18 P3B4	
D00761	proteasome component C5; macropain subunit C5	0.5	2.4	1.6	1.0	1.6	1.3	1.3	1.1	1.5	0.6	0.9	0.2801
L06139	angiopoietin 1 receptor precursor; TIE-2	2.1	2.3	2.4	0.6	0.8	2.0	1.4	1.3	1.2	1.3	0.8	0.0986
U09577	LUCA2; lysosomal hyaluronidase 2 (HYAL2)	2.4	2.0	2.5	1.3	1.2	2.0	1.2	1.1	2.2	1.0	1.1	0.0258
M80359	p78 putative serine/threonine-protein kinase	2.3	2.9	1.6	1.3	1.6	1.9	2.3	1.1	1.6	1.5	0.5	0.0132
M28215	ras-related protein RAB5A	1.8	4.0	1.9	1.4	2.1	1.4	1.5	1.4	1.7	0.6	0.6	0.0449
M34664	heat shock protein 60 (HSP-60)	2.4	3.5	2.0	1.0	1.2	1.7	2.8	1.4	1.1	0.8	0.5	0.1228
M13228	N-myc proto-oncogene	2.4	3.6	1.7	1.5	2.3	1.7	0.9	0.9	1.3	1.3	0.3	0.2831
X67951	thioredoxin-dependent peroxide reductase 2	1.8	1.7	2.1	2.2	1.1	1.6	1.3	2.2	1.4	0.9	1.3	0.0538
M14648	vitronectin receptor alpha subunit; integrin alpha 5 subunit	1.9	1.9	2.3	2.1	1.2	1.8	0.8	1.6	1.3	0.9	1.0	0.1649
M73780	integrin beta 8 precursor (ITGB8)	1.6	2.1	1.9	1.8	1.1	1.1	0.7	1.4	1.1	0.7	0.7	0.2170
X63465	rap1 GTPase-GDP dissociation stimulator 1	1.2	1.7	2.2	1.8	1.0	1.6	1.0	1.2	1.7	1.1	1.1	0.2155
M21574	platelet-derived growth factor receptor alpha subunit (PDGFRA)	1.6	1.3	1.4	1.1	1.5	0.6	0.7	1.2	1.8	0.9	0.7	0.2155
U51478	sodium/potassium-transporting ATPase beta 3 subunit	1.9	0.2	1.7	1.8	1.9	2.0	1.5	0.4	1.0	0.6	1.2	0.2831
X06234	migration inhibitory factor-related protein 8; calgranulin A	1.2	0.9	2.8	3.1	2.4	1.0	1.1	2.2	1.9	0.7	2.8	0.2170
U26662	neuronal pentraxin II precursor (NP2)	0.7	0.5	2.5	2.3	2.2	1.0	1.0	2.4	1.9	0.6	2.1	0.1228
M14764	low-affinity nerve growth factor receptor	1.0	1.2	2.3	3.7	1.8	1.0	0.6	2.4	1.5	0.9	1.5	0.0641
X51602	vascular endothelial growth factor receptor 1 (VEGFR1)	5.8	2.7	3.9	6.0	1.4	2.3	1.8	2.5	1.8	2.2	1.8	0.0206
M64673	heat shock factor protein 1 (HSF1)	2.2	1.6	2.0	1.8	0.8	1.5	1.5	1.7	1.3	0.8	1.5	0.0449
D90209	cAMP-dependent transcription factor ATF-4; CREB2 *	1.8	1.3	1.9	1.8	0.7	1.4	1.5	1.5	1.4	1.1	1.6	0.1427
M32977	vascular endothelial growth factor precursor (VEGF)	2.3	1.9	5.8	4.2	1.4	1.1	1.5	3.2	1.1	1.7	3.2	0.0372

Table 2. *Genes differentially expressed in NAWM.* List of differentially expressed genes with median differences of 1.5 folds or more in NAWM of more than half of the MS cases. Upregulation is shown in red, whereas downregulation is shown in green. Genes were grouped according to their cluster localization shown in Figure 2A. Medians of ratios against all control samples are shown for each MS sample. The statistical significance is expressed as p-value determined by the non-parametric Mann-Whitney U-Test. *P*-values below 0.05 are shown in yellow.

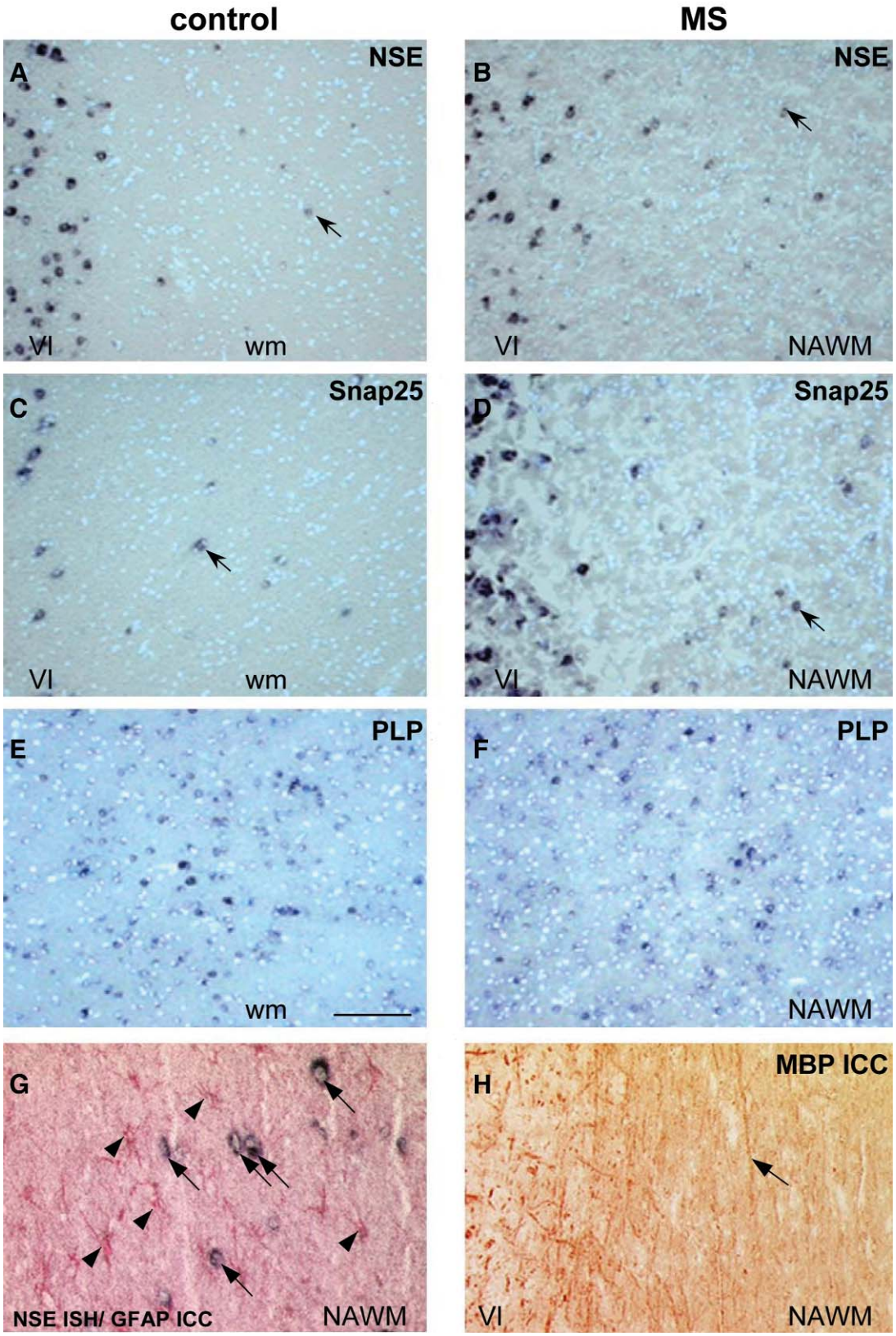
control
MS
A
NSE
VI
wm
B
NSE
VI
NAWM
C
Snap25
VI
wm
D
Snap25
VI
NAWM
E
PLP
wm
F
PLP
NAWM
G
NSE ISH/ GFAP ICC
NAWM
H
MBP ICC
VI
NAWM

comparable expression pattern between control and NAWM tissue (Figure 4E, F) supporting our RT-PCR analysis (Figure 3A).

Cluster analysis of differentially expressed genes in NAWM. Sorting of the differentially expressed genes in NAWM by their expression pattern within the MS cases revealed 4 clusters with highest significance in Cluster I and II (Table 2). We detected upregulation of Snap25, synaptophysin, RAB3A, presynaptic density protein 95 (PSD95), and distinct types of glutamate receptors such as the NMDA receptor 2B and the metabotropic glutamate receptor mGLUR5. We also detected upregulation of genes of the GABA system such as glutamate decarboxylase GAD67 and the GABA B receptor 1A, and 2 as well as GABA A receptor gamma-2. In addition, genes involved in metabolic homeostasis such as the brain glucose transporter 3, taurine transporter and ion transporters such as the Na^+/K^+-transporting ATPα1 and sodium/hydrogen exchanger 1 were significantly upregulated. Although most of the trophic factors were normally expressed, TGFβ2 was significantly upregulated. Within this cluster, upregulation of the thyroid hormone and the trkB receptors was also evident, as well as the transcription factors Krox24, CREB/ATF2 and hepatic leukemia factor (HLF). Stress related genes such as glycogen synthase kinase 3beta (GSK3) and the NO receptor guanylate cyclase beta-1 were also significantly upregulated.

Cluster II represents the largest gene group analyzed, and within this cluster 3 subgroups could be identified. Interestingly, in Cluster IIA HIF1α and genes it induces, such as PDGF-B, transferrin receptor and insulin growth factor binding protein 1 (IGFBP1) are found (Tables 2, 3A). Additionally, genes encoding for proteins involved in signal transduction, such as LIMK-1, CAMKI, adenomatous poliposis coli protein (APC), insulin growth factor 1 receptor (IGF1R), ski oncogene and snoN were significantly upregulated. In Cluster IIB many genes involved in macrophage attraction are represented (eg, EMAPII, MCSF). In addition, FKBP-rapamycin-associated protein (FRAP), neuropeptide Y and the transcription factor activating the endothelin promoter DB1 are localized in this cluster. In cluster IIC, upregulation of PI3K and the receptors for PDGFB, FGF, EGF and IL-6 are depicted. Of considerable interest is the finding that Cluster II contains genes encoding for DNA repair enzymes (eg, xeroderma pigmentosa, REF-1) and the different members of the free radical scavenger system, glutathione-S-transferase.

In Cluster III some inflammation related genes such as ICAM1, TNFR1, MCP-1, LFA-1, and CSF-1-R are localized. Within this cluster a significant upregulation of hypoxanthine-guanine phosphoribosyltransferase, an enzyme important for the pyridine nucleotide metabolism, was observed.

In Cluster IV, genes related to vascular endothelial cells (eg, VEGF and VEGF receptor 1) and the heat shock factor protein 1 (HSF1) were detected.

Death promoting genes, including the caspases and death associated protein kinase 1 as well as anti-apoptotic regulating genes, eg, 14-3-3, BAG-1, bcl-x and bcl-w, are significantly upregulated and distributed throughout the different clusters. Two forms of calpains, proteases known to be involved in calcium-depending degradation and indicators of oxidative stress, are also found to be upregulated in the major MS group (Cluster IIC and III).

One striking observation from array II and III was the strong upregulation of the 2 neurofilament isoforms NF-L and NF-M as well as the neuron specific growth associated protein SCG10 in MS1, MS3, MS5, MS10 and MS26 (data not shown).

Discussion

The pathological hallmark of MS is the demyelinated plaque. The molecular and cellular mechanisms involved in lesion formation are still unknown. Most studies have concentrated on the characterization of actively demyelinating inflammatory lesions and little is known about molecular and cellular changes in the so-called pre-plaque tissue. To investigate alterations in transcriptional regulation that could lead to lesion for-

Figure 4. (Opposing page) *Localization of neurons in sub-cortical white matter.* In situ hybridisation of NSE (**A, B, G**), Snap25 (**C, D**) and PLP (**E, F**) were performed on fresh frozen tissue sections from control (**A, C, E**) and MS brain tissues (**B, D, F, G**). NSE and Snap25 are highly expressed in neurons of layer VI and in subcortical white matter (arrows). Colocalization studies (**G**) with NSE in situ hybridisation (blue, arrows) and GFAP immunohistochemistry (red, arrowheads) showed localization of neurons in subcortical NAWM of a MS case distant to cortical grey matter layer VI; note, no colocalization of NSE-expressing cells with GFAP immunohistochemistry (ICC) was observed. Fluorescent counterstaining with Hoechst detected all nuclei (white). (H) shows myelinated fibers (arrow as an example) by immunohistochemistry for MBP of a representative cortical tissue block of a MS case delineating layer VI in grey matter from subcortical white matter. In situ hybridization of PLP (**E, F**) shows a comparable number of oligodendrocytes in control white matter and NAWM. Abbreviations: wm, white matter; NAWM, normal appearing white matter. Bar in **E**: for **A-F**, **H** = 132 μm; **G** = 33.7 μm.

A. Induced by HIF-1α

Gene Bank Accession	Gene	p-value	Cluster
M20681	Brain glucose transporter 3 (GTR3) (39)	0.0208	I
M29645	Insulin-like growth factor 2 (IGF2) (39)	0.0693	I
K03015	Neuroleukin; glucose-6-phosphate isomerase (31)	0.0043	IIA
X01060	Transferrin receptor (TFRC) (39)	0.0258	IIA
X02811	Platelet-derived growth factor B subunit (PDGF B) (16)	0.0105	IIA
M31145	Insulin-like growth factor binding protein 1 (IGFBP1) (39)	0.0069	IIA
X02751	N-ras; transforming p21 protein (39)	0.2472	IIA
M29870	P21-rac1 (39)	0.0034	IIA
K03195	Erythrocyte glucose transporter 1(GLUT1) (39)	0.0896	IIA
M32977	Vascular endothelial growth factor (VEGF) (39)	0.0372	IV
X51602	Vascular endothelial growth factor receptor 1 (VEGFR1) (39)	0.0206	IV
M75126	Hexokinase1 (HK1) (39)	0.0176	Array II

B. Induced by hypoxia

Gene Bank Accession	Gene	p-value	Cluster
Z18956	Sodium-chloride-dependent taurine transporter (TAUT) (35)	0.0258	I
J04111	C-jun proto-oncogene; transcription factor AP-1 (16)	0.0641	I
X52541	Early growth response protein 1 (hEGR1); Krox24 (16)	0.0055	I
U08839	Urokinase-type plasminogen activator receptor (U-PAR) (16)	0.0390	I
M31630	cAMP response element binding protein (CRE-BP1), ATF2 (16)	0.0390	I
M32865	Ku 70-kDa subunit; ATP-dependent DNA helicase 2 (16)	0.0208	I
U22431	Hypoxia-inducible factor 1 alpha (HIF-1α) (16)	0.0168	IIA
S40706	Growth arrest & DNA-damage-inducible protein 153 (GADD153) (16)	0.0012	IIA
L05515	cAMP-responsive element-binding protein (CREB1) (16)	0.1649	IIB
X54936	Placenta growth factors 1 + 2 (PLGF1 + PLGF2) (16)	0.2477	IIC
X59764	DNA-(apurinice or apyridinic site) lyase; AP endonuclease 1 (16)	0.0475	IIC
X57766	Matrix metalloproteinase 11 (MMP11); stromelysin 3 (16)	0.1266	IIC
X53586	Integrin alpha 6; VLA6 (16)	0.3637	IIC
M24545	Monocyte chemotactic protein 1 (MCP1) (16)	0.1427	III
U09579	Cyclin-dependent inhibitor 1; WAF1 (16)	0.2472	III
U41766	Metalloprotease/ disintegrin/ cystein-rich protein (MDC9) (16)	0.3280	III
L06139	Angiopoetin 1 receptor; TIE-2 (16)	0.0986	IV
M64673	Heat shock factor protein 1 (HSF1) (16)	0.0449	IV
M14648	Vitronectin receptor alpha subunit; integrin alpha 5 subunit (16)	0.1649	IV
AB004066	DEC1 (16)	0.0285	Array II
BC002745	Neuron specific enolase (NSE) (12, 21)	0.0006	LC

C. Involved in preconditioning pathways

Gene Bank Accession	Gene	p-value	Cluster
AF056085	GABA-B receptor 2 subunit (GABA-BR2) (22, 29)	0.0082	I
Y11044	GABA-B receptor 1A subunit (GABA-BR1A) (22, 29)	0.0087	I
X65293	Protein kinase C epsilon type (NPKC-ε) (4, 37)	0.0475	I
U07236	Proto-oncogen tyrosine-protein kinase lck (4)	0.0132	I
M25269	Elk-1; ETS-related proto-oncogen (30)	0.1864	I
M31630	cAMP response element binding protein (CRE-BP1), ATF2 (30)	0.0390	I
U08316	Ribosomal S6 kinase 2 (RSK2) (30)	0.0166	I
U59747	Apoptosis regulator bclw; BCL2L2 (30)	0.0208	I
X59932	C-src kinase (CSK) (4)	0.1167	I
U24152	P21-activated kinase alpha (PAK1) (38)	0.0132	I
U90278	Glutamate (NMDA) receptor subunit epsilon 2 (NMDAR2B) (30)	0.0575	I
U83192	Presynaptic density protein 95 (PSD95) (30)	0.0390	I
U22431	Hypoxia-inducible factor 1 alpha (HIF-1α) (30, 39)	0.0168	IIA
X03484	c-raf proto-oncogen (30)	0.0829	IIA
X02751	N-ras; transforming p21 protein (30)	0.2472	IIA
L05624	MAPKK1; ERK activated kinase 1 (37)	0.0132	IIA
L29511	Growth factor receptor-bound protein 2 (GRB2) (9)	0.0136	IIA
M29870	P21-rac1 (38)	0.0034	IIA
L35253	Mitogen-activated protein kinase p38 (MAPkinase p38) (37)	0.0641	IIA
U12779	MAP kinase-activated protein kinase 2 (MAPKAPK-2) (37)	0.0575	IIA
L05515	cAMP-responsive element-binding protein (CREB1) (17, 30)	0.1649	IIB
Z23115	Apoptosis regulator bclx (44)	0.0055	IIB
X85106	Ribosomal S6 kinase 3 (RSK3) (30)	0.1372	IIB
M84489	Extracellular signal-regulated kinase 2 (ERK2; p42-MAPK) (37)	0.0206	IIC
S56143	Adenosine A1 receptor (ADORA1) (37)	0.1228	IIC
M61906	Phosphatidyl 3-kinase regulatory alpha subunit (37)	0.0449	IIC
X76981	Adenosine A3 receptor (ADORA3) (37)	0.1864	III

mation or protect against it, we performed expression profiling of sub-cortical NAWM of MS brain tissue and control white matter using microarray technology.

The present study has revealed the upregulation of a significant number of genes in NAWM of MS brains. This appears to involve the upregulation of genes that reflect a higher energy metabolism as well as genes involved in endogenous neuroprotection, which may affect all neural cell types. Of particular importance is the finding of an upregulation of genes known to be induced upon oxidative stress and the triggering of long-term ischemic preconditioning. This is best illustrated by the upregulation of the transcription factor HIF1α, CREB, the associated members of the PI3K/Akt signalling pathway, and their target genes such as VEGF, VEGF receptor1, hexokinase 1 and the glucose 3 transporter (Figure 5A; Table 3A). A general neuroprotective reaction against oxidative stress is suggested by the upregulation of the sodium and chloride dependent taurine transporter (35), adenosine A1 receptor (18) and GABA-A/B receptors (22) (Figure 5B; Table 3C). The induction of genes involved in protection mechanisms against apoptosis, such as 14-3-3, and in DNA repair mechanisms also support our hypothesis. In keeping with the histological analysis, molecular signs of active inflammation were not evident, yet upregulation of STAT6 in all MS cases may indicate that the residing macrophages/microglia in the normal appearing tissue in MS may be persistently activated. In contrast, little evidence was found of astrogliosis in the NAWM.

MS is a chronic progressive disease with repetitive influx of inflammatory cells into the CNS. This leads to changes in the cerebral vascular endothelium as well as nervous tissue damage due to release of various inflammatory mediators. Mediators such as IL-1, TNFα and reactive oxygen and nitrogen species (ROS/RNS) are suggested to be involved in the pathophysiology of MS (6, 42). Yet, in NAWM we found the induction of regulatory components involved in long-term ischemic preconditioning. Preconditioning against oxidative stress is induced by sublethal insults such as hypoxia, endotoxins, IL-1, TNFα, ROS/RNS and adenosine, and protects against subsequent lethal ischemic attacks (4). In NAWM of MS tissues the persistent presence of activated macrophages/microglia could be one of the sources of ROS and RNS. It is notable that they have been found to produce more ROS than cells from controls (42). The deleterious effects of free radicals on the functional properties of myelin and axons in inflammatory demyelinated MS lesions are well described (for review see 42). Nitric oxide and its derivatives are cytotoxic, impair respiratory chain function and can cause axonal conduction block, to which demyelinated axons are more susceptible (42). Oligodendrocytes and neurons are more sensitive to free radical-mediated damage than astrocytes or microglia (27). Immature oligodendrocytes, which arise from progenitors following demyelination and become involved in remyelination, show an increased vulnerability to ROS due to their high demand for iron during myelination. This could lead to increased iron uptake via transferrin receptors, which are upregulated in NAWM. In situations of iron overload and low plasma pH that occur during oxidative stress, transferrin releases bound iron, and chelatable forms of Fe can escape sequestration in biological systems producing free radicals via the Fenton reaction. The free radicals may release even more iron by mobilizing it from ferritin (23, 46). Iron release and free radical production combined with relative low levels of antioxidant defense may lead to extensive cell damage (20). The low GSH levels in oligodendrocytes and neurons may predetermine a higher risk of lipid peroxidation. However, in most of our analyzed NAWM tissues we observed upregulation of several glutathione-S-transferases, which may indicate a protective mechanism against oxidative stress (34). Interestingly, the patient without pathological lesions in the brain (MS18) showed a rather "normal" expression pattern compared to those with lesions. However, several genes which are induced upon oxidative stress were upregulated (eg, brain glucose transporter 3, the sodium- and chloride-dependent taurine transporter, ICAM1 and VEGF). In addition, in this case the presence of activated macrophages/microglia was indicated by upregulation of MCSF and STAT6 which correlates well with our immunohistochemical data showing CD68 positive cells throughout the NAWM (data not shown).

Our analysis also uncovered the upregulation of many genes involved in neuronal function (Table 2). The upregulation of genes involved in axonal transport and synaptic transmission suggests functional alterations in neurons of the subcortical white matter in MS. In contrast to other mammalian species, neurons in the subcortical white matter in humans persist throughout life

Table 3. (Opposing page) *Differential expression of genes in NAWM related to oxidative stress.* List of genes known to be induced by HIF-1α (**A**), or by hypoxia (**B**) or are involved in preconditioning pathways (**C**) and which are upregulated in NAWM are summarized. References are indicated for each gene.

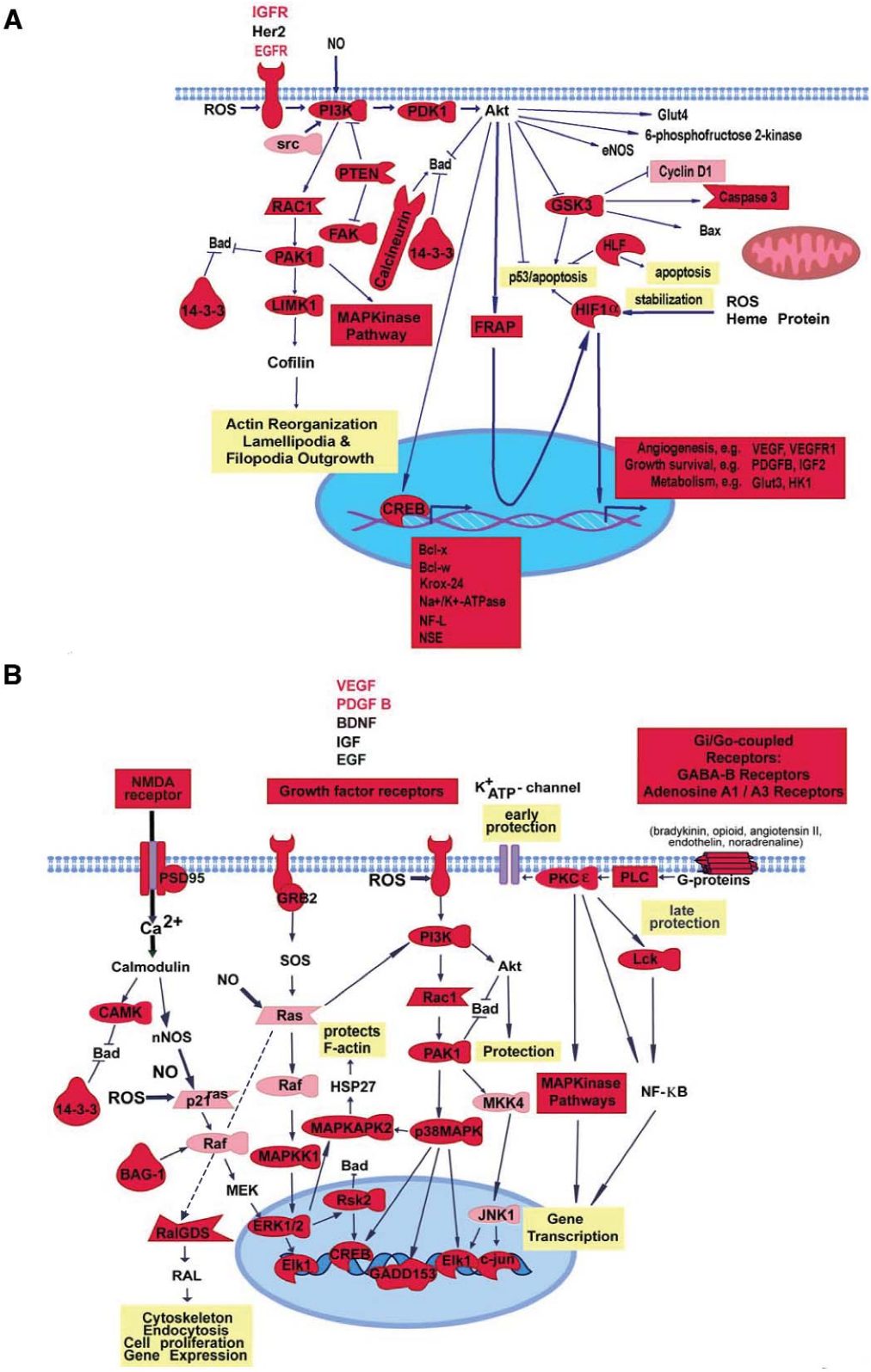
A
IGFR
Her2
EGFR
NO
ROS
PI3K
PDK1
Akt
Glut4
6-phosphofructose 2-kinase
eNOS
src
PTEN
Bad
Cyclin D1
Caspase 3
RAC1
FAK
Calcineurin
14-3-3
GSK3
Bax
Bad
PAK1
HLF
apoptosis
p53/apoptosis
14-3-3
LIMK1
MAPKinase Pathway
FRAP
stabilization
HIF1α
ROS
Heme Protein
Cofilin
Actin Reorganization
Lamellipodia &
Filopodia Outgrowth
Angiogenesis, e.g. VEGF, VEGFR1
Growth survival, e.g. PDGFB, IGF2
Metabolism, e.g. Glut3, HK1
CREB
Bcl-x
Bcl-w
Krox-24
Na+/K+-ATPase
NF-L
NSE
B
VEGF
PDGF B
BDNF
IGF
EGF
Gi/Go-coupled Receptors:
GABA-B Receptors
Adenosine A1 / A3 Receptors
NMDA receptor
Growth factor receptors
K+ATP- channel
early protection
(bradykinin, opioid, angiotensin II, endothelin, noradrenaline)
PSD95
GRB2
ROS
PKCε
PLC
G-proteins
late protection
Ca2+
PI3K
Lck
Calmodulin
SOS
Akt
NO
Rac1
CAMK
Ras
Bad
nNOS
protects F-actin
PAK1
Protection
Bad
NO
Raf
HSP27
MAPKinase Pathways
NF-κB
14-3-3
ROS
p21ras
MKK4
MAPKAPK2
p38MAPK
Raf
MAPKK1
BAG-1
Bad
MEK
Rsk2
JNK1
Gene Transcription
RalGDS
ERK1/2
Elk1
CREB
GADD153
Elk1
c-jun
RAL
Cytoskeleton
Endocytosis
Cell proliferation
Gene Expression

and comprise both non-pyramidal inhibitory GABAergic neurons, expressing neuropeptide Y, somatostatin and vasoactive intestinal polypeptide (VIP), and also small numbers of glutaminergic pyramidal neurons that receive a thalamic input (8, 28). Alterations in transcriptional regulation in these neurons in subcortical NAWM may indicate a compensatory mechanism for stabilizing normal function, but may also suggest a predisposition towards axonal dysfunction leading finally to axonal loss, which has been described in NAWM (3, 14). Indeed, recent microarray studies of demyelinated lesions showed downregulation of neuronal genes such as GAP43, SCG10, synaptophysin, NF-L and NF-M (24), which were either not affected (eg, GAP43) or upregulated in our study (Table 2, cluster 1).

The most important finding of this study was the upregulation of gene expression in a number of signaling pathways related to oxidative stress and ischemic preconditioning. Two of the pathways are induced by activation of growth factor receptors signalling via MAPkinase (10, 38, 44) (Figure 5B). The activation of G protein-coupled receptors could induce short-term as well as long-term protection (33, 37) (Figure 4B). Preconditioning in neurons is dependent upon activation of the N-methyl-D-aspartate (NMDA) glutamate receptor leading to Ca^{2+}-influx and NO-production (15, 30) (Figure 5B). In addition, almost all members of the PI3/Akt-pathway were upregulated, which would be expected to protect against apoptosis (7, 38), and lead to the transcription of HIF1α (40) (Figure 5A). HIF-1α has been reported to suppress apoptosis in mild hypoxic experimental conditions (32, 43) and induces genes encoding proteins that mediate adaptive responses to reduced oxygen availability (39, 40) (Table 3A). It is to note that these growth factor receptor mediated signalling pathways do also play a vital role in oligodendrocyte survival. Their upregulation might indicate an increased effort to maintain oligodendrocyte function and myelin maintenance as well. Thus, we propose that in MS NAWM a balance has developed between oxidative stress and protective mechanisms. These mechanisms may counteract lesion formation to some extent, but do not abolish disease progression. This is in line with the very recent observation that hypoxia-like white matter damage was detected in a subtype of MS cases (1). Indeed, in these cases nuclear localization of HIF1α in oligodendrocytes was observed. Microarray studies of demyelinating lesions, however, did not reveal differential expression of HIF-1α and its induced genes (Table 3), with the exception of rac-1, which was downregulated (24), suggesting that ischemic preconditioning is not taking place in demyelinating lesions or has not been detected due to the low expression levels of the corresponding genes.

Our data clearly show that in MS the brain is mounting a global defense against oxidative stress in order to preserve cellular function, even in areas remote from active inflammatory and demyelinating lesions. Novel therapeutic treatments could address either supporting the ongoing endogenous autoprotective mechanism and/or inactivating the downstream deleterious effects of the oxidative stress. New therapeutic strategies can now take into account preconditioning as a major mechanism for neuroprotection in MS. An increased understanding of the underlying mechanisms of preconditioning against ROS /RNS could be exploited to develop more specific treatment to protect the different resident cell types and thus minimize progressive oligodendrocyte and axonal loss.

Acknowledgments

We thank B. Erne, J. Caduff, S. Zaugg and A. Graham for technical support. G. De Libero (Department of Research, University Hospital Basel, Switzerland), P. Magistretti (Institute of Physiology, University of Lausanne, Switzerland) and Ph. Lyrer (Neurology Department, University Hospital Basel, Switzerland) are thanked for helpful discussions and critical reading of the manuscript. MS and control tissue samples were supplied by the UK Multiple Sclerosis Tissue Bank, funded by the Multiple Sclerosis Society of Great Britain and Northern Ireland (registered charity 207495). Diagnostic confirmation of the UK cases was carried out by M. Graeber. We also thank A. Probst and M. Tolnay (Neuropathology, University Hospital Basel, Switzerland) for supplying post-mortem control brain tissues. This study was supported by grants from the Swiss Multiple

Figure 5. (Opposing page) *Schematic overview of the different pathways proposed to be upregulated in MS NAWM.* Preconditioning pathways leading to gene transcription in long-lasting protection against oxidative stress are shown. Symbols in red indicate significantly upregulated genes and in pink upregulated in some MS cases. Panel (**A**) summarizes the different PI3K signalling pathways leading to HIF1α (39, 40) and CREB (26) transcriptional regulation as well as other down stream effects via Akt (7, 10) and LIM kinase (19). Neuronal preconditioning pathways via the NMDA-receptor (30) and GABA-B receptors (22) as well as adenosine receptors (18) are described in Panel (**B**). Furthermore, preconditioning pathways via activation of growth factor receptors (10, 38, 44, 45) and other G-protein coupled receptors were described in myocardium (4, 33, 37).

Sclerosis Society, the French MS Society (ARSEP) and the UK MS Society (grant 619/01).

References

1. Aboul-Enein F, Rauschka H, Kornek B, Stadelmann C, Stefferl A, Bruck W, Lucchinetti C, Schmidbauer M, Jellinger K, Lassmann H. (2003) Preferential loss of myelin-associated glycoprotein reflects hypoxia-like white matter damage in stroke and inflammatory brain diseases. *J Neuropathol Exp Neurol* 62:25-33.
2. Allen IV, McKeown SR. (1979) A histological, histochemical and biochemical study of the macroscopically normal white matter in multiple sclerosis. *J Neurol Sci* 41:81-91.
3. Bjartmar C, Kinkel RP, Kidd G, Rudick RA, Trapp BD. (2001) Axonal loss in normal-appearing white matter in a patient with acute MS. *Neurology* 57:1248-1252.
4. Bolli R. (2000) The late phase of preconditioning. *Circ Res* 87:972-983.
5. Bothwell A, Yancopoulos GD, Alt FW. (1990) Methods for cloning and analysis of eukaryontic genes. Jones and Bartlett, Boston.
6. Brosnan CF, Raine CS. (1996) Mechanisms of immune injury in multiple sclerosis. *Brain Pathol* 6:243-257.
7. Chen EY, Mazure NM, Cooper JA, Giaccia AJ. (2001) Hypoxia activates a platelet-derived growth factor receptor/phosphatidylinositol 3-kinase/Akt pathway that results in glycogen synthase kinase-3 inactivation. *Cancer Res* 61:2429-2433.
8. Chun JJ, Shatz CJ. (1989) Interstitial cells of the adult neocortical white matter are the remnant of the early generated subplate neuron population. *J Comp Neurol* 282:555-569.
9. Cullen PJ, Lockyer PJ. (2002) Integration of calcium and Ras signalling. *Nat Rev Mol Cell Biol* 3:339-348.
10. Datta SR, Dudek H, Tao X, Masters S, Fu H, Gotoh Y, Greenberg ME. (1997) Akt phosphorylation of BAD couples survival signals to the cell-intrinsic death machinery. *Cell* 91:231-241.
11. Eisen MB, Spellman PT, Brown PO, Botstein D. (1998) Cluster analysis and display of genome-wide expression patterns. *Proc Natl Acad Sci U S A* 95:14863-14868.
12. Farwell W, Simonyi A, Scott H, Zhang JP, Carruthers V, Madsen R, Johnson J, Sun GY. (1998) Effects of ischemic tolerance on mRNA levels of IP3R1, beta-actin, and neuron-specific enolase in hippocampal CA1 area of the gerbil brain. *Neurochem Res* 23:539-542.
13. Filippi M, Campi A, Dousset V, Baratti C, Martinelli V, Canal N, Scotti G, Comi G. (1995) A magnetization transfer imaging study of normal-appearing white matter in multiple sclerosis. *Neurology* 45:478-482.
14. Fu L, Matthews PM, De Stefano N, Worsley KJ, Narayanan S, Francis GS, Antel JP, Wolfson C, Arnold DL. (1998) Imaging axonal damage of normal-appearing white matter in multiple sclerosis. *Brain* 121:103-113.
15. Gonzalez-Zulueta M, Feldman AB, Klesse LJ, Kalb RG, Dillman JF, Parada LF, Dawson TM, Dawson VL. (2000) Requirement for nitric oxide activation of p21(ras)/extracellular regulated kinase in neuronal ischemic preconditioning. *Proc Natl Acad Sci U S A* 97:436-441.
16. Harris AL. (2002) Hypoxia—a key regulatory factor in tumour growth. *Nat Rev Cancer* 2:38-47.
17. Hazzalin CA, Mahadevan LC. (2002) MAPK-regulated transcription: a continuously variable gene switch? *Nat Rev Mol Cell Biol* 3:30-40.
18. Heurteaux C, Lauritzen I, Widmann C, Lazdunski M. (1995) Essential role of adenosine, adenosine A1 receptors, and ATP-sensitive K+ channels in cerebral ischemic preconditioning. *Proc Natl Acad Sci U S A* 92:4666-4670.
19. Jaffer ZM, Chernoff J. (2002) p21-activated kinases: three more join the Pak. *Int J Biochem Cell Biol* 34:713-717.
20. Juurlink BH. (1997) Response of glial cells to ischemia: roles of reactive oxygen species and glutathione. *Neurosci Biobehav Rev* 21:151-166.
21. Karkela J, Bock E, Kaukinen S. (1993) CSF and serum brain-specific creatine kinase isoenzyme (CK-BB), neuron-specific enolase (NSE) and neural cell adhesion molecule (NCAM) as prognostic markers for hypoxic brain injury after cardiac arrest in man. *J Neurol Sci* 116:100-109.
22. Lee JM, Grabb MC, Zipfel GJ, Choi DW. (2000) Brain tissue responses to ischemia. *J Clin Invest* 106:723-731.
23. Lesnefsky EJ. (1994) Tissue iron overload and mechanisms of iron-catalyzed oxidative injury. *Adv Exp Med Biol* 366:129-146.
24. Lock C, Hermans G, Pedotti R, Brendolan A, Schadt E, Garren H, Langer-Gould A, Strober S, Cannella B, Allard J, Klonowski P, Austin A, Lad N, Kaminski N, Galli SJ, Oksenberg JR, Raine CS, Heller R, Steinman L. (2002) Gene-microarray analysis of multiple sclerosis lesions yields new targets validated in autoimmune encephalomyelitis. *Nat Med* 8:500-508.
25. Lucchinetti C, Bruck W, Parisi J, Scheithauer B, Rodriguez M, Lassmann H. (2000) Heterogeneity of multiple sclerosis lesions: implications for the pathogenesis of demyelination. *Ann Neurol* 47:707-717.
26. Mayr B, Montminy M. (2001) Transcriptional regulation by the phosphorylation-dependent factor CREB. *Nat Rev Mol Cell Biol* 2:599-609.
27. Merrill JE, Scolding NJ. (1999) Mechanisms of damage to myelin and oligodendrocytes and their relevance to disease. *Neuropathol Appl Neurobiol* 25:435-458.
28. Meyer G, Wahle P, Castaneyra-Perdomo A, Ferres-Torres R. (1992) Morphology of neurons in the white matter of the adult human neocortex. *Exp Brain Res* 88:204-212.
29. Mironov SL, Richter DW. (2000) Intracellular signalling pathways modulate K(ATP) channels in inspiratory brainstem neurones and their hypoxic activation: involvement of metabotropic receptors, G-proteins and cytoskeleton. *Brain Res* 853:60-67.
30. Nandagopal K, Dawson TM, Dawson VL. (2001) Critical role for nitric oxide signaling in cardiac and neuronal ischemic preconditioning and tolerance. *J Pharmacol Exp Ther* 297:474-478.

31. Niizeki H, Kobayashi M, Horiuchi I, Akakura N, Chen J, Wang J, Hamada JI, Seth P, Katoh H, Watanabe H, Raz A, Hosokawa M. (2002) Hypoxia enhances the expression of autocrine motility factor and the motility of human pancreatic cancer cells. *Br J Cancer* 86:1914-1919.
32. Piret JP, Mottet D, Raes M, Michiels C. (2002) Is HIF-1alpha a pro- or an anti-apoptotic protein? *Biochem Pharmacol* 64:889-892.
33. Rubino A, Yellon DM. (2000) Ischaemic preconditioning of the vasculature: an overlooked phenomenon for protecting the heart? *Trends Pharmacol Sci* 21:225-230.
34. Sagara J, Sugita Y. (2001) Characterization of cytosolic glutathione S-transferase in cultured astrocytes. *Brain Res* 902:190-197.
35. Saransaari P, Oja SS. (1999) Characteristics of ischemia-induced taurine release in the developing mouse hippocampus. *Neuroscience* 94:949-954.
36. Schaeren-Wiemers N, Gerfin-Moser A. (1993) A single protocol to detect transcripts of various types and expression levels in neural tissue and cultured cells: in situ hybridization using digoxigenin-labelled cRNA probes. *Histochemistry* 100:431-440.
37. Schulz R, Cohen MV, Behrends M, Downey JM, Heusch G. (2001) Signal transduction of ischemic preconditioning. *Cardiovasc Res* 52:181-198.
38. Seko Y, Takahashi N, Tobe K, Kadowaki T, Yazaki Y. (1997) Hypoxia and hypoxia/reoxygenation activate p65PAK, p38 mitogen-activated protein kinase (MAPK), and stress-activated protein kinase (SAPK) in cultured rat cardiac myocytes. *Biochem Biophys Res Commun* 239:840-844.
39. Semenza GL. (2001) Hypoxia-inducible factor 1: oxygen homeostasis and disease pathophysiology. *Trends Mol Med* 7:345-350.
40. Semenza GL. (2002) HIF-1 and tumor progression: pathophysiology and therapeutics. *Trends Mol Med* 8:S62-67.
41. Silver NC, Tofts PS, Symms MR, Barker GJ, Thompson AJ, Miller DH. (2001) Quantitative contrast-enhanced magnetic resonance imaging to evaluate blood-brain barrier integrity in multiple sclerosis: a preliminary study. *Mult Scler* 7:75-82.
42. Smith KJ, Kapoor R, Felts PA. (1999) Demyelination: the role of reactive oxygen and nitrogen species. *Brain Pathol* 9:69-92.
43. Suzuki H, Tomida A, Tsuruo T. (2001) Dephosphorylated hypoxia-inducible factor 1alpha as a mediator of p53-dependent apoptosis during hypoxia. *Oncogene* 20:5779-5788.
44. Walton MR, Dragunow I. (2000) Is CREB a key to neuronal survival? *Trends Neurosci* 23:48-53.
45. Wick A, Wick W, Waltenberger J, Weller M, Dichgans J, Schulz JB. (2002) Neuroprotection by hypoxic preconditioning requires sequential activation of vascular endothelial growth factor receptor and Akt. *J Neurosci* 22:6401-6407.
46. Ying W, Han SK, Miller JW, Swanson RA. (1999) Acidosis potentiates oxidative neuronal death by multiple mechanisms. *J Neurochem* 73:1549-1556.